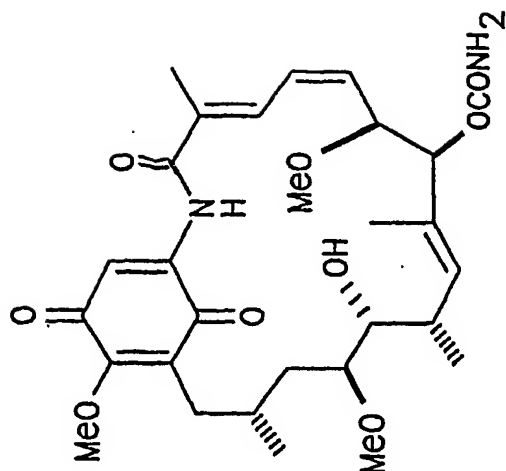
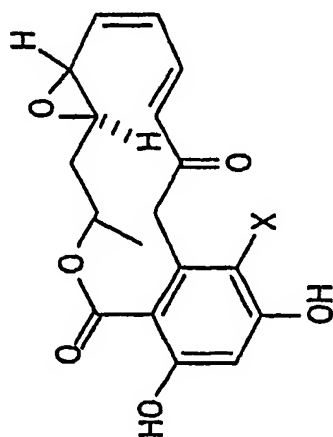


1/39

FIG. 1



Geldanamycin (3)



X=Cl Radical (1)

X=H Monocillin I (2)

FIG. 2

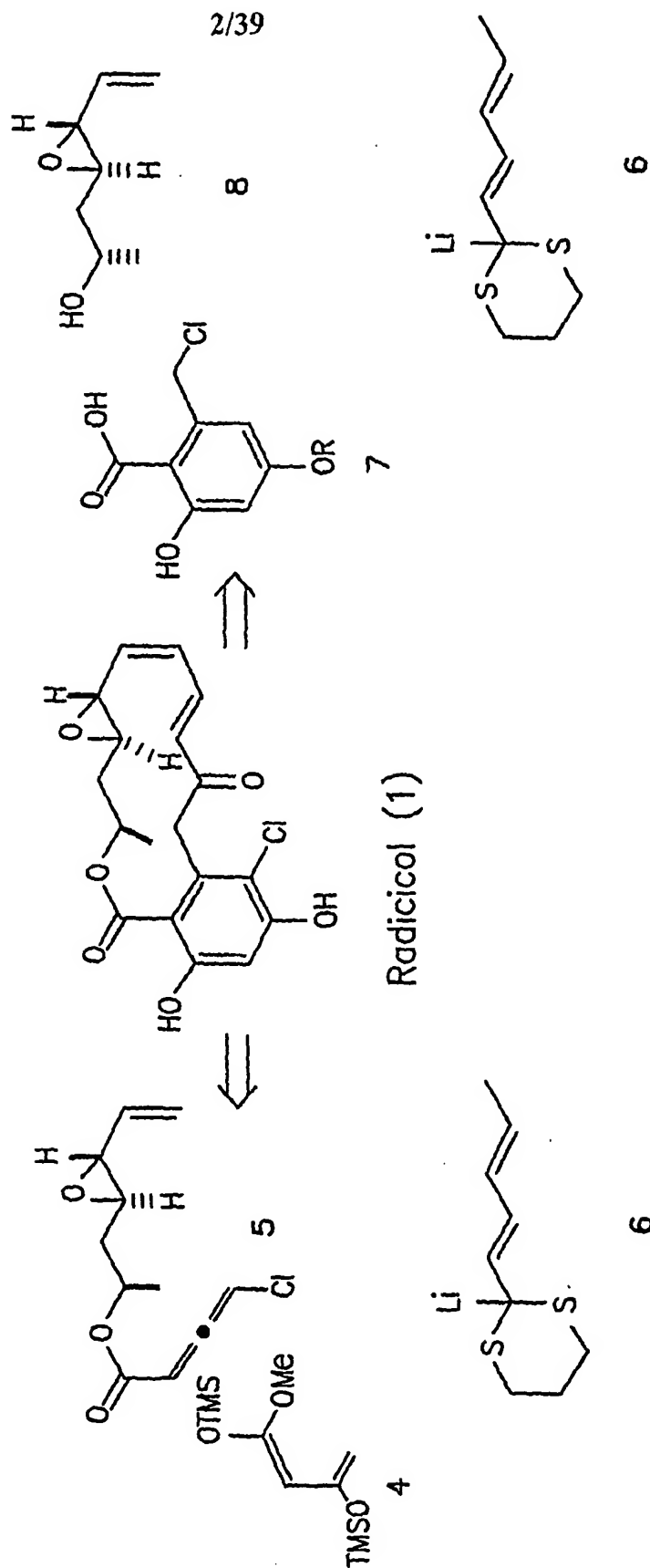
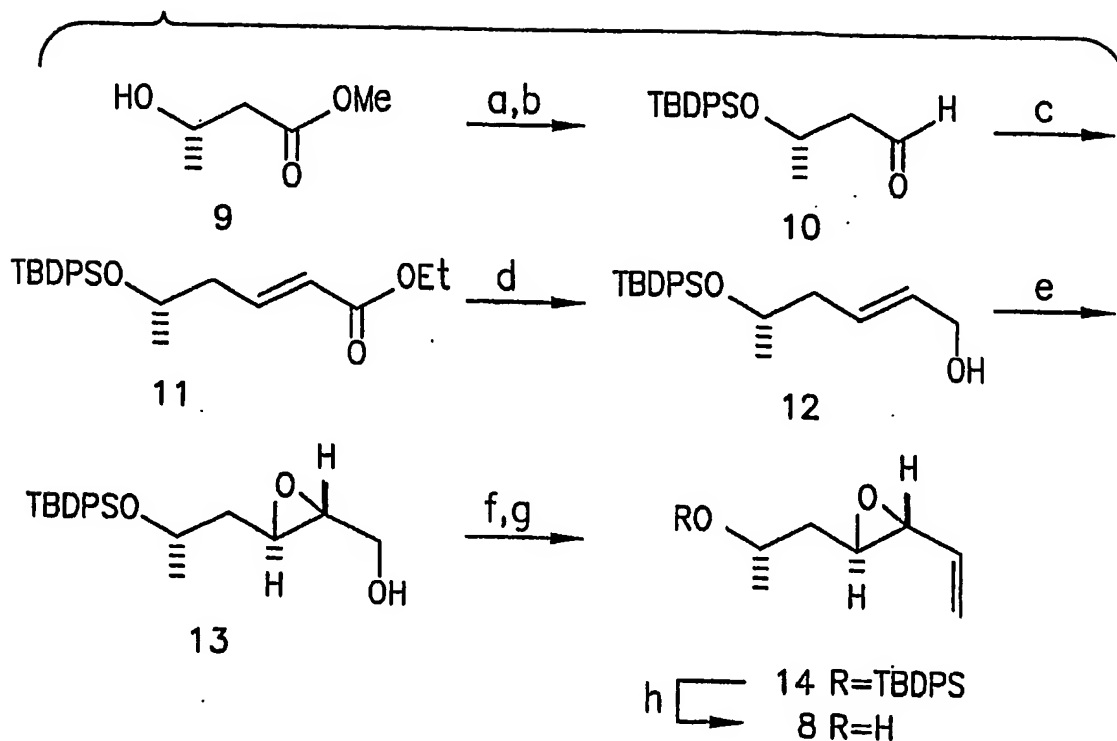


FIG. 3

3/39



- (a) TBDPSCI, imid., >95%; (b) DIBAL-H, -78 °C, 92%;
 (c) LiCl, DIPEA (EtO)₂P(O)CH₂CO₂Et, 95%;
 (d) DIBAL-H, -20 °C, 96%; (e) (+)-DET, Ti(OiPr)₄, TBHP, 90%, >95% ee; (f) SO₃*pyridine, Et₃N, DMSO, 90%;
 (g) PH₃PCH₃Br, NaHMDS, 0 °C, 82%; (h) TBAF, 89%.

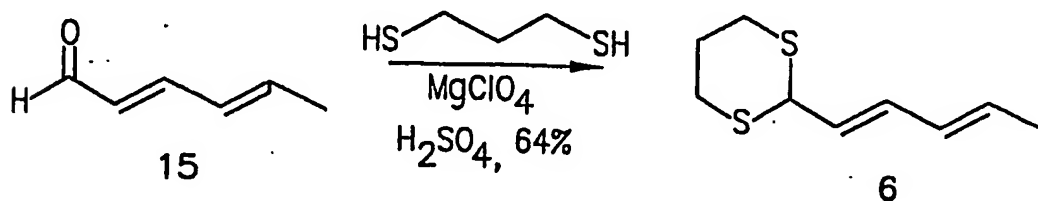
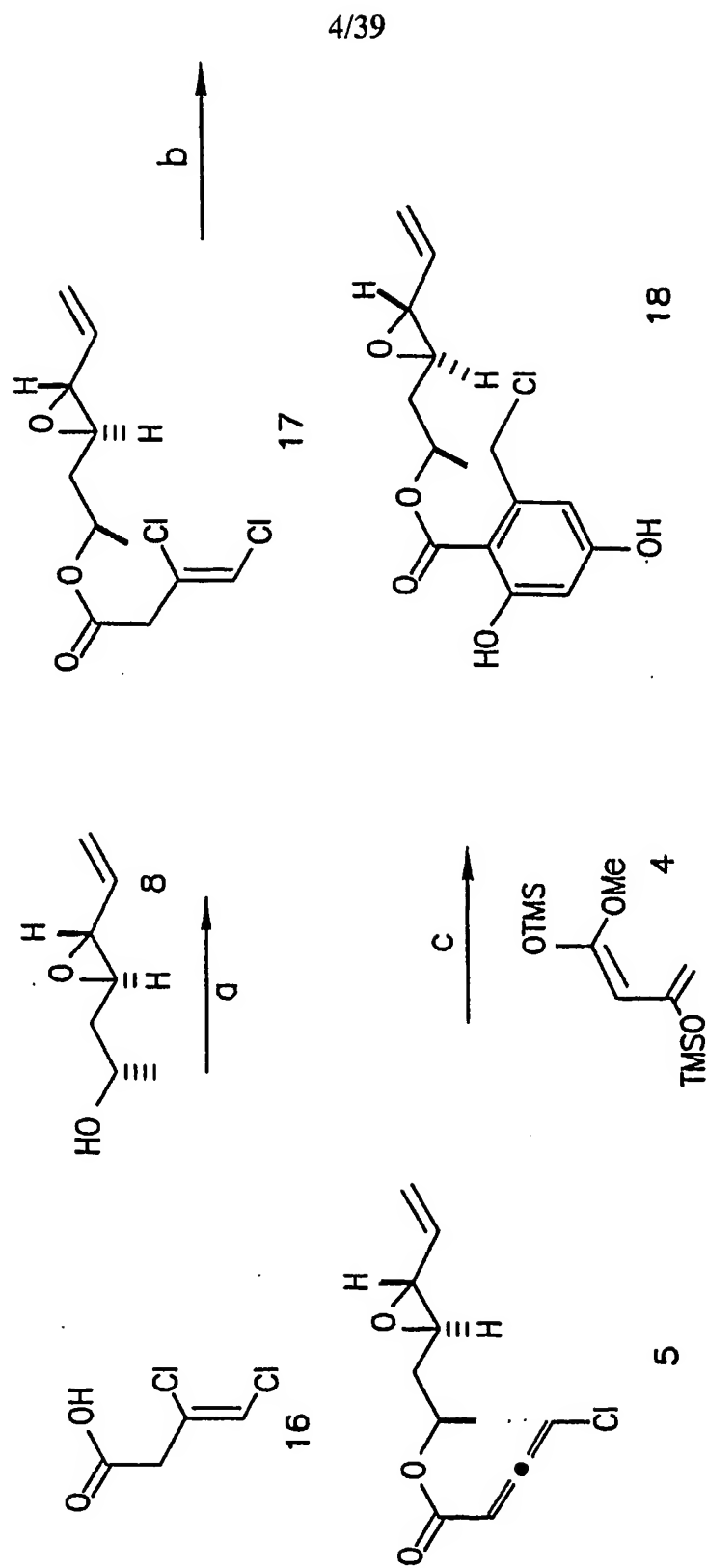
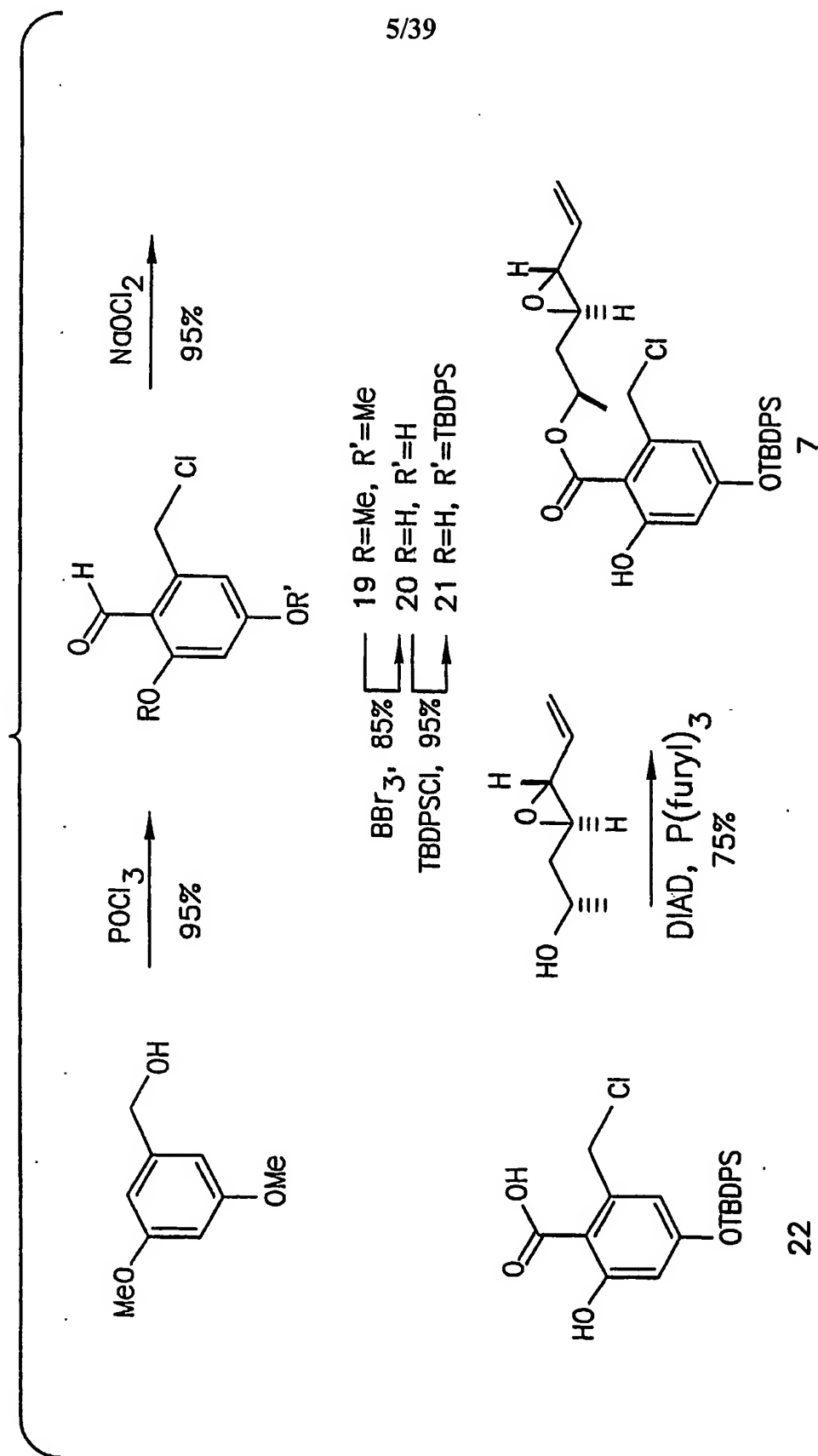


FIG. 4



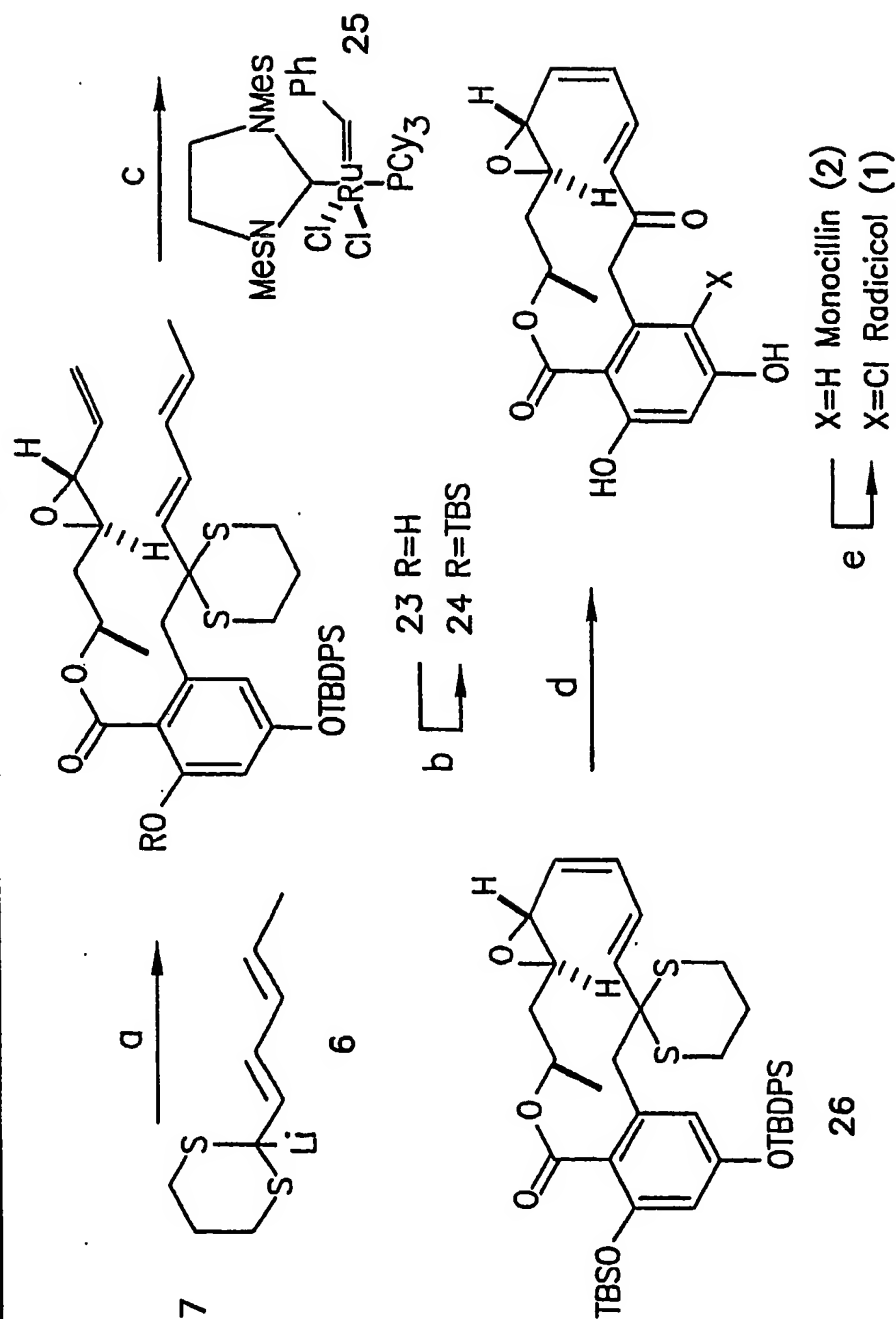
(a) DEAD, PPh₃, 70%; (b.) iPr₂NEt, 70%; (c.) 50% (4:1)

FIG. 5



6/39

FIG. 6



a. *n*-BuLi, -78 °C, 50% (6:1); b. TBSCl, 83%; c. 42 °C, 70%; d. (i) mCPBA, (ii) Ac₂O, Et₃N, H₂O, 60 °C, (iii) NaHCO₃, MeOH, 60%; e. SO₂Cl₂, 50%

FIG. 7

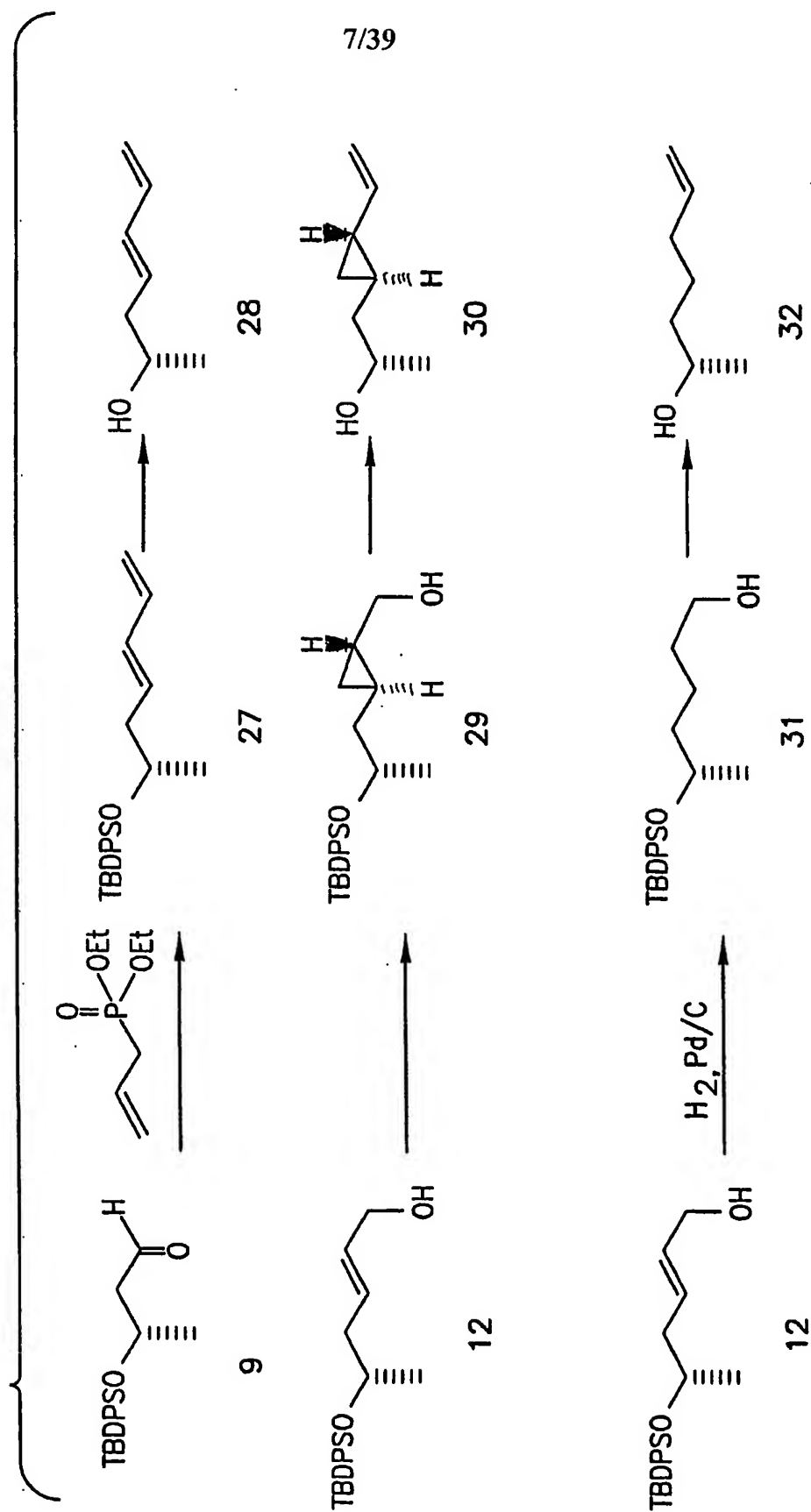


FIG. 8

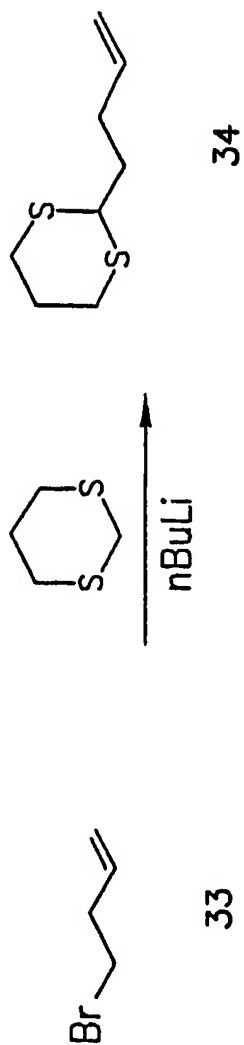


FIG. 9

9/39

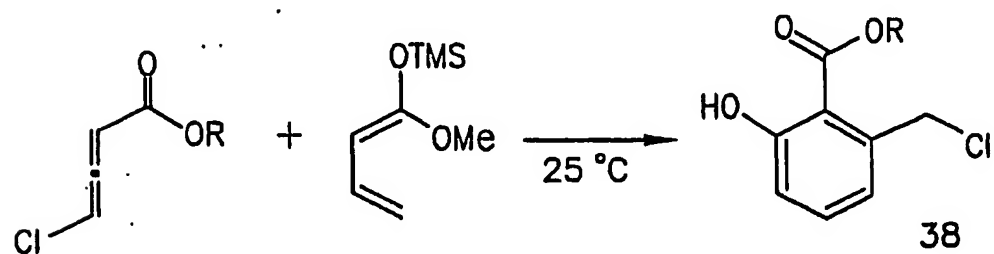
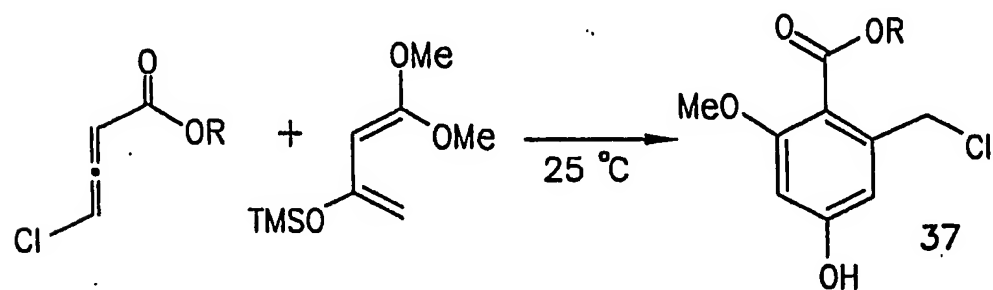
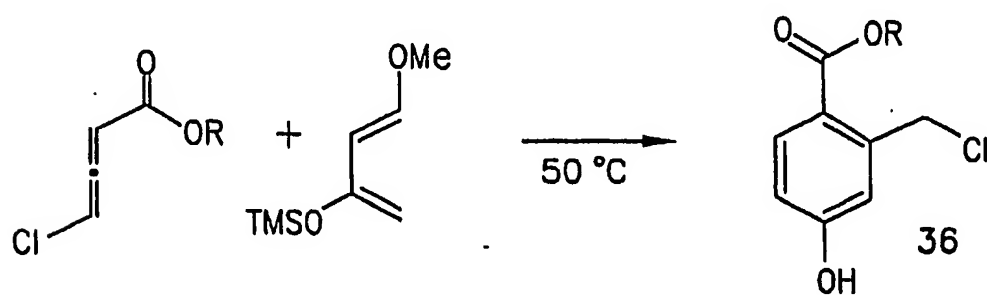
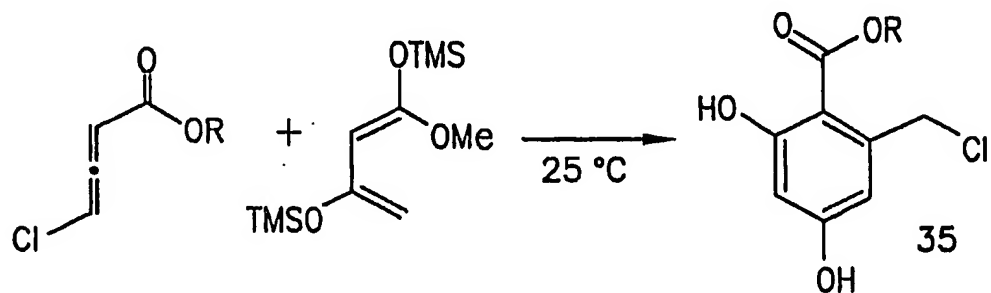
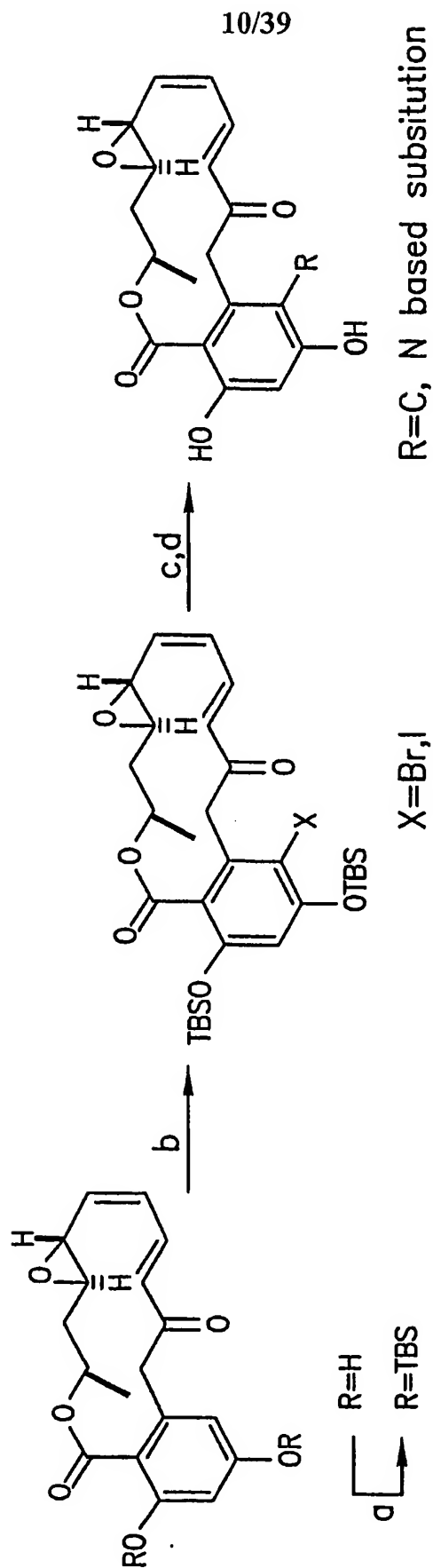
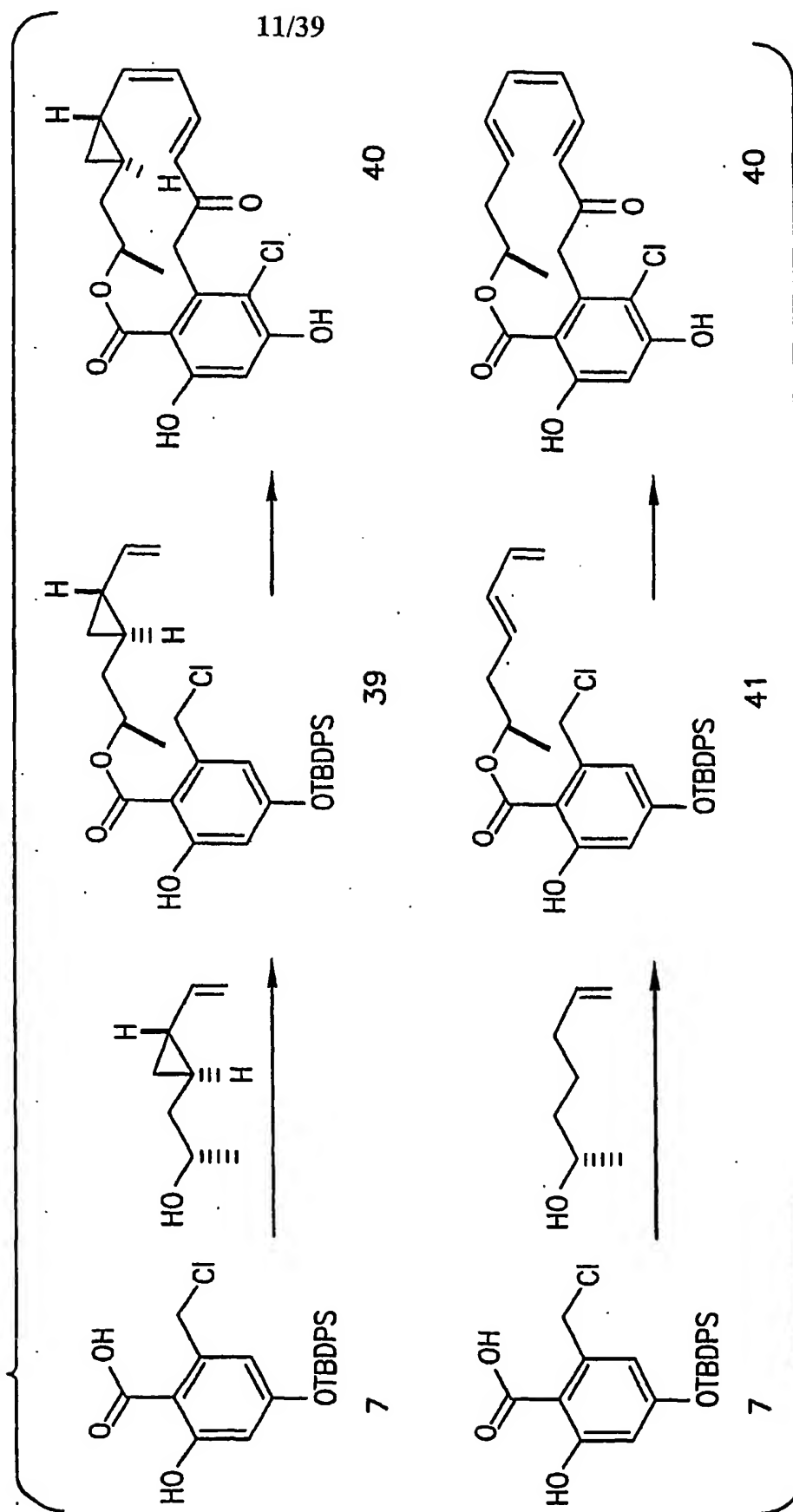


FIG. 10



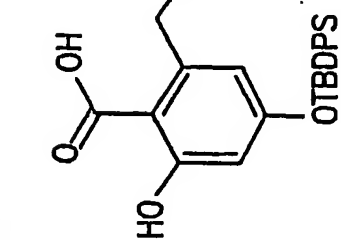
a. TBSCl, pyridine; b. NIS or NBS, TsOH; c. $\text{Pd}(\text{PPh})_3$, $\text{R}(\text{SnBu}_3)_3$, $\text{d. nBu}_4\text{NF}$

FIG. 11-1

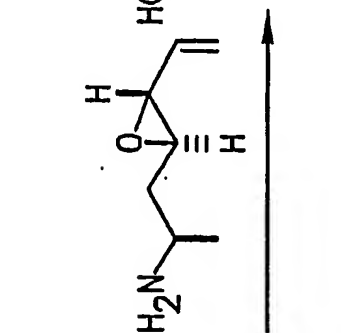


FROM FIG. 11-1

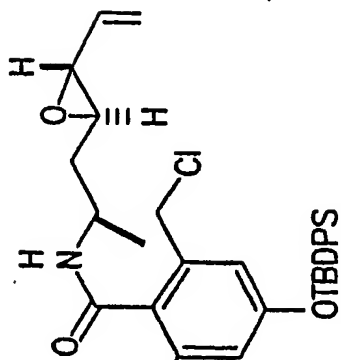
FIG. 11-2



7

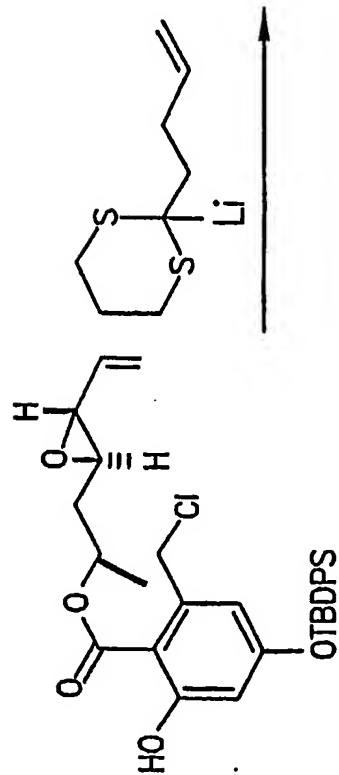


39

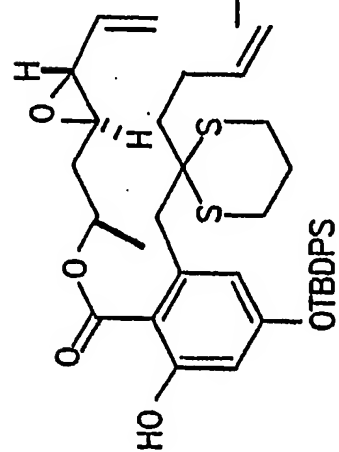


44

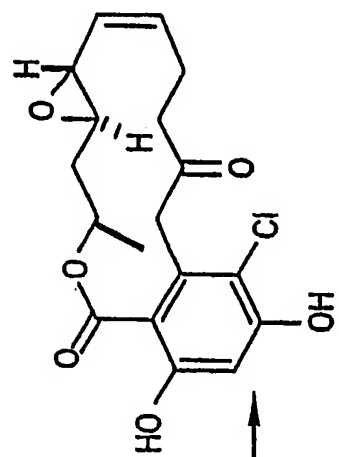
12/39



22

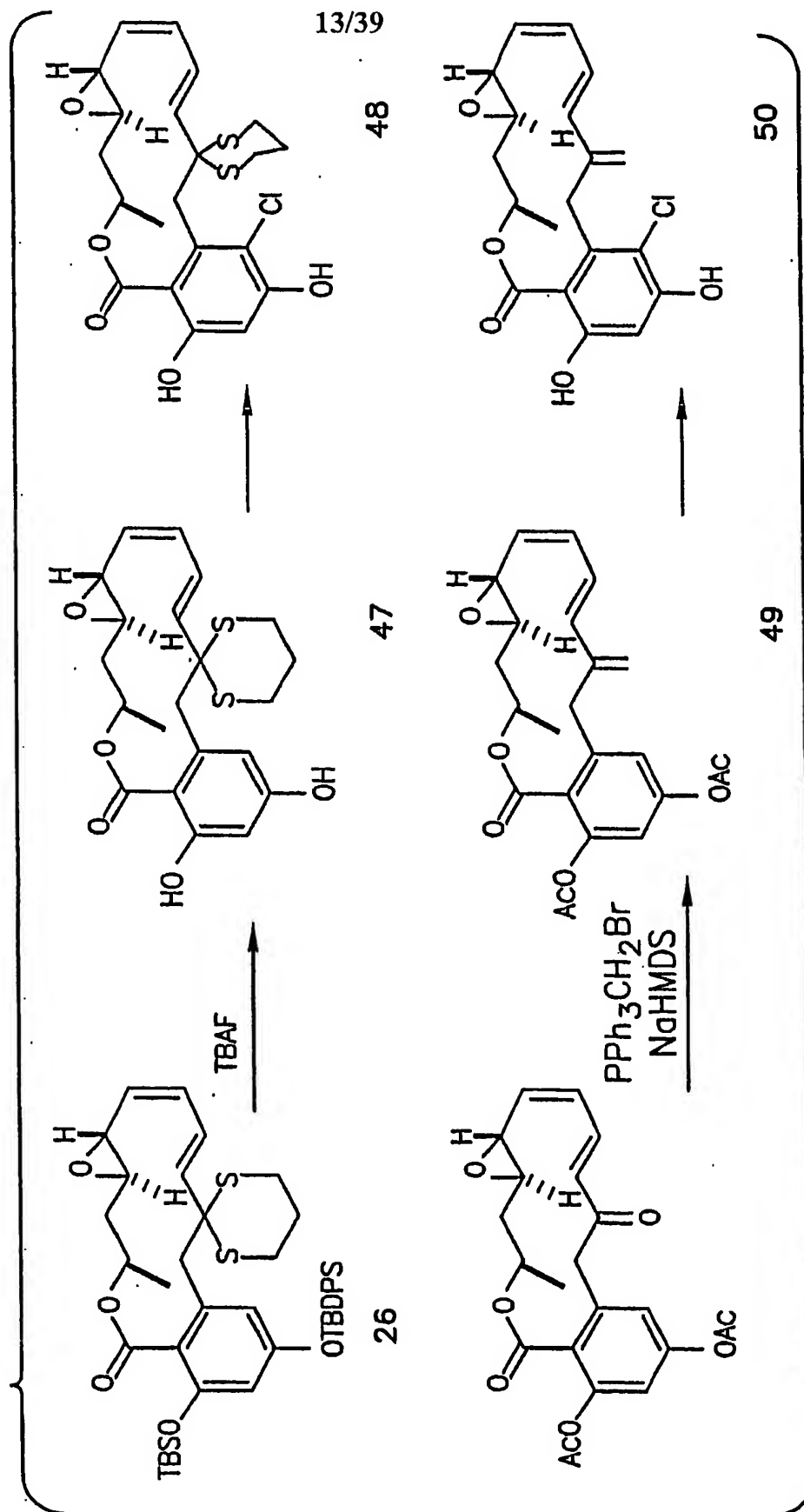


45



46

FIG. 12-1



FROM FIG. 12-1

FIG. 12-2

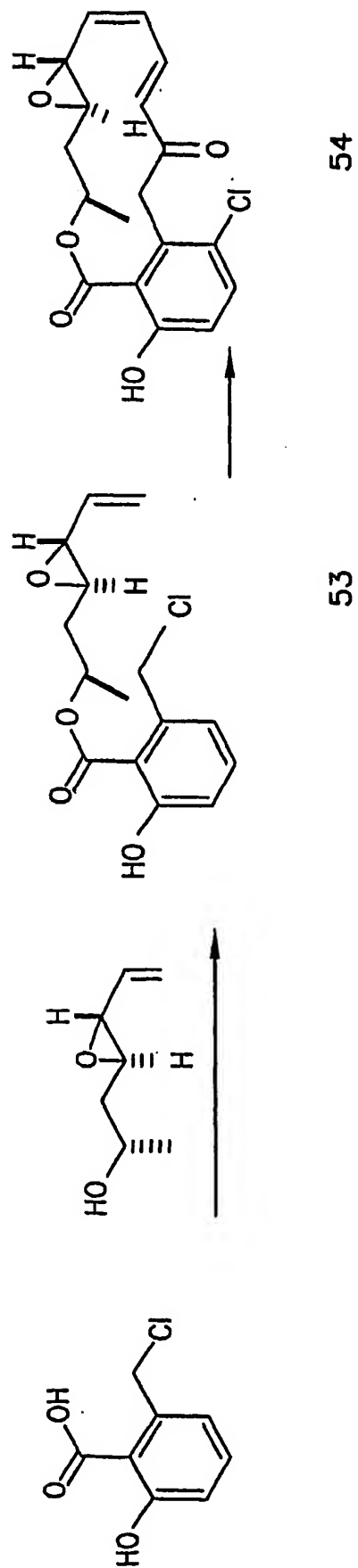
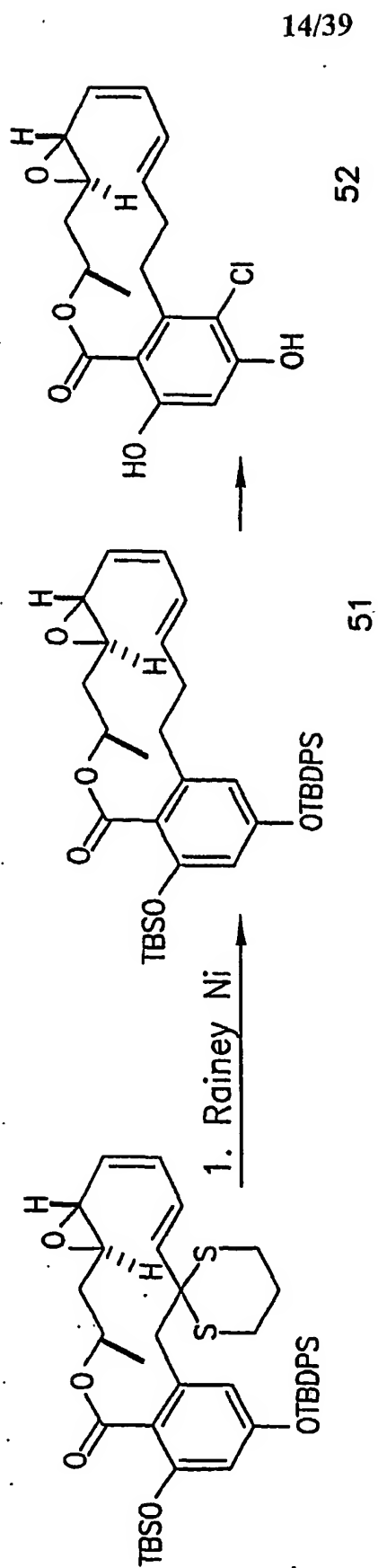
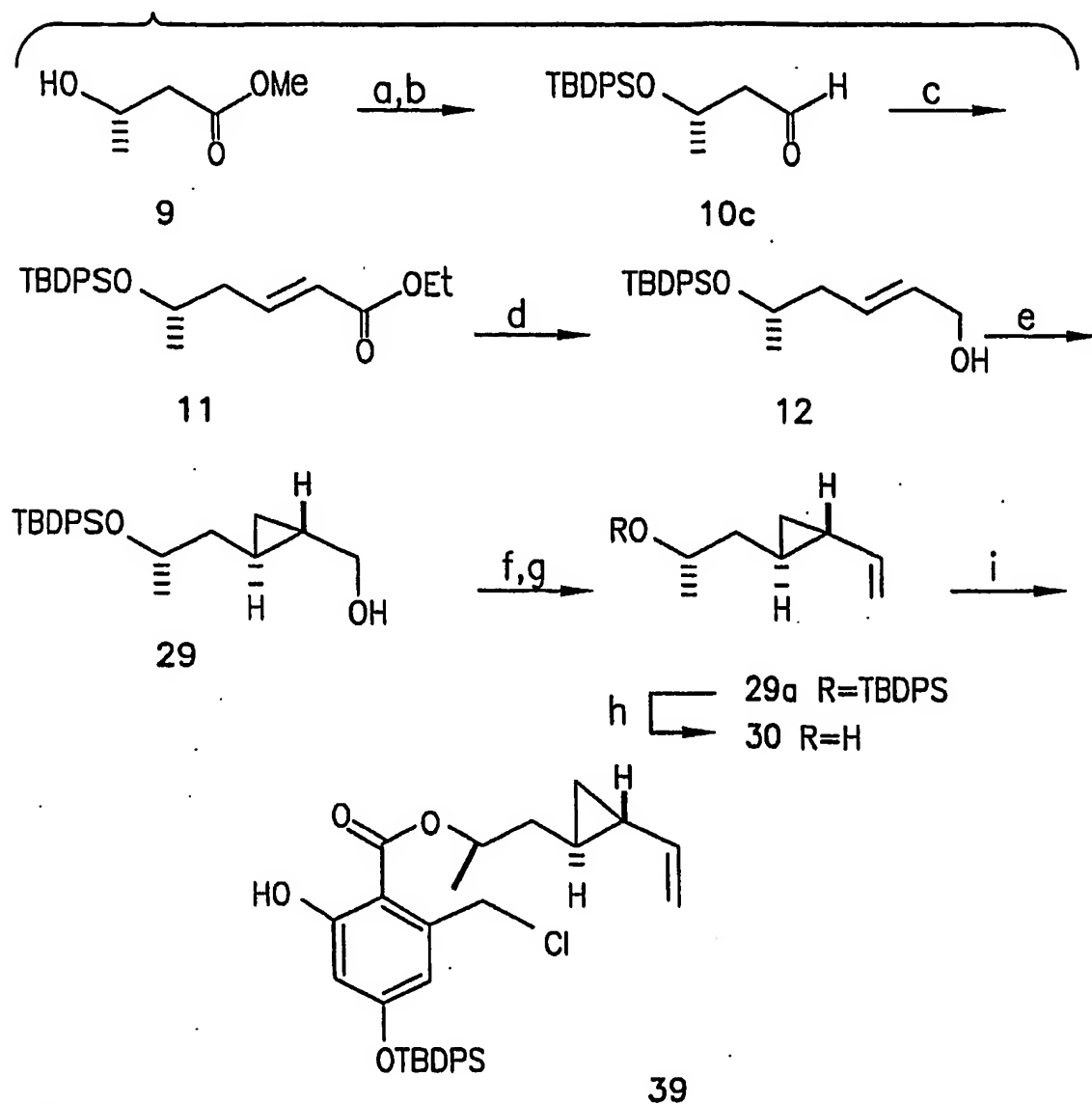


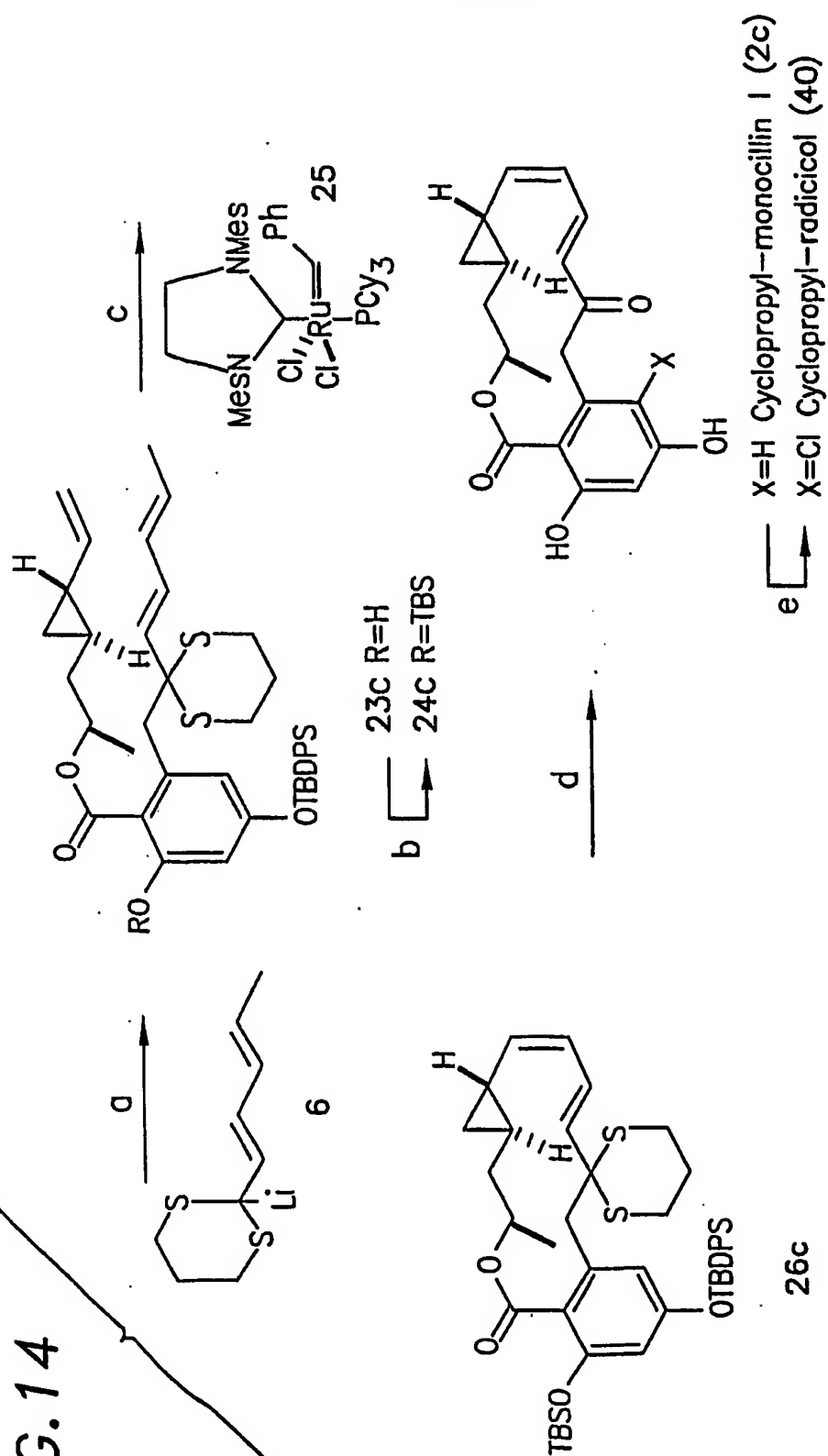
FIG. 13

15/39



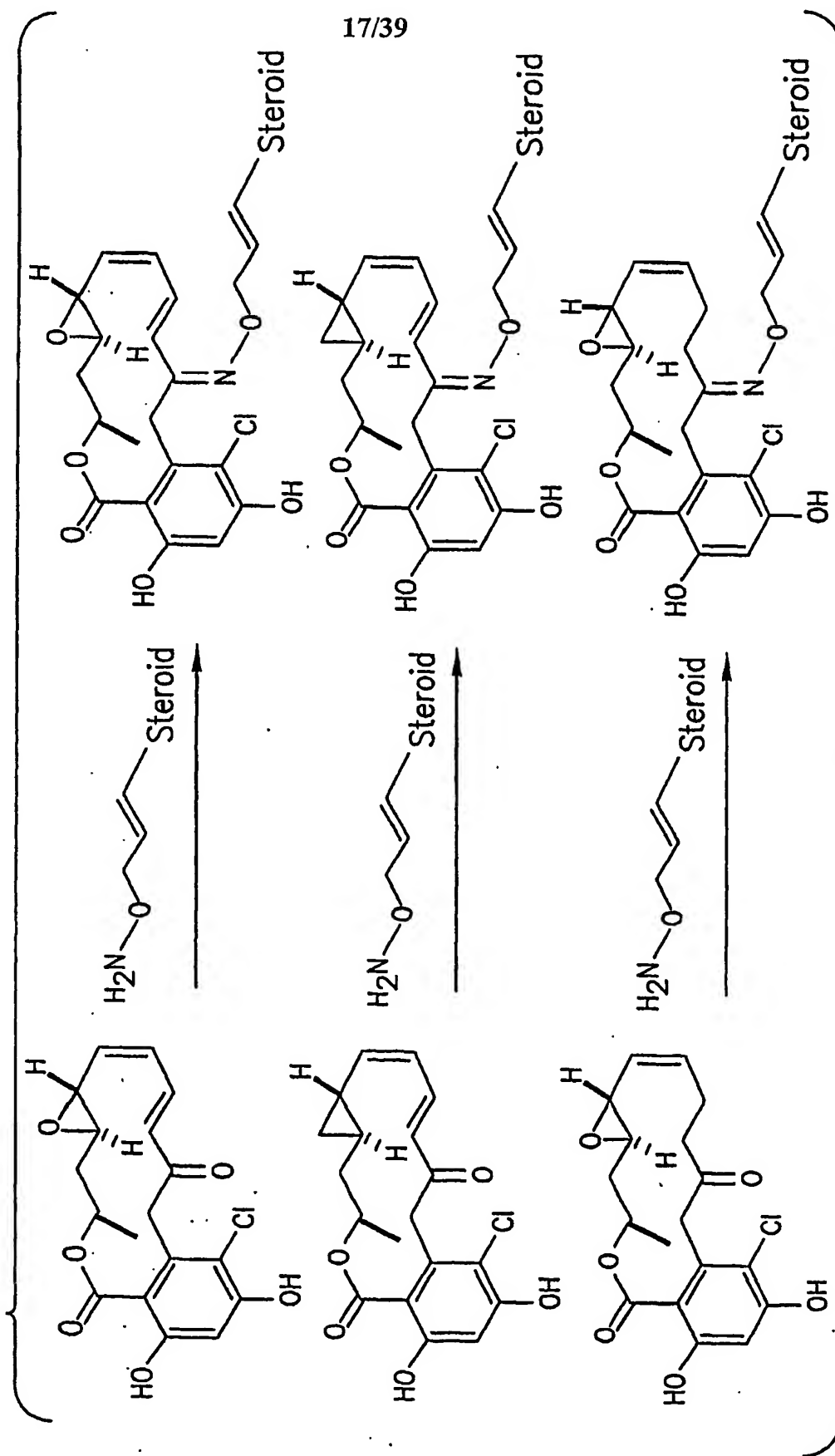
^a (a) TBDPSCI, imid., >95%; (b) DIBAL-H, -78 °C, 92%; (c) LiCl, DIPEA (EtO)₂P(O)CH₂CO₂Et, 95%; (d) DIBAL-H -20 °C, 96%; (e) (+)-tetramethyltartaric acid diamide-BBu, Et₂Zn, CH₂I₂, 9 >95% ee; (f) SO₃*pyridine, Et₃N, DMSO, 90%; (g) Ph₃PCH NaHMDS, 0 °C, 82%; (h) TBAF, 89%; (i) 7, P(furyl)₃, DIA benzene, 60%

16/39



a. $n\text{-BuLi}$, -78°C , 75% (3:1); b. TBSCl, 83%; c. 42°C , 20%; d. (i) mCPBA, (ii) Ac_2O , Et_3N , H_2O , 60°C , (iii) NaHCO_3 , MeOH, 60%; e. SO_2Cl_2 , 80%

FIG. 15-1



FROM FIG. 15-1

FIG. 15-2

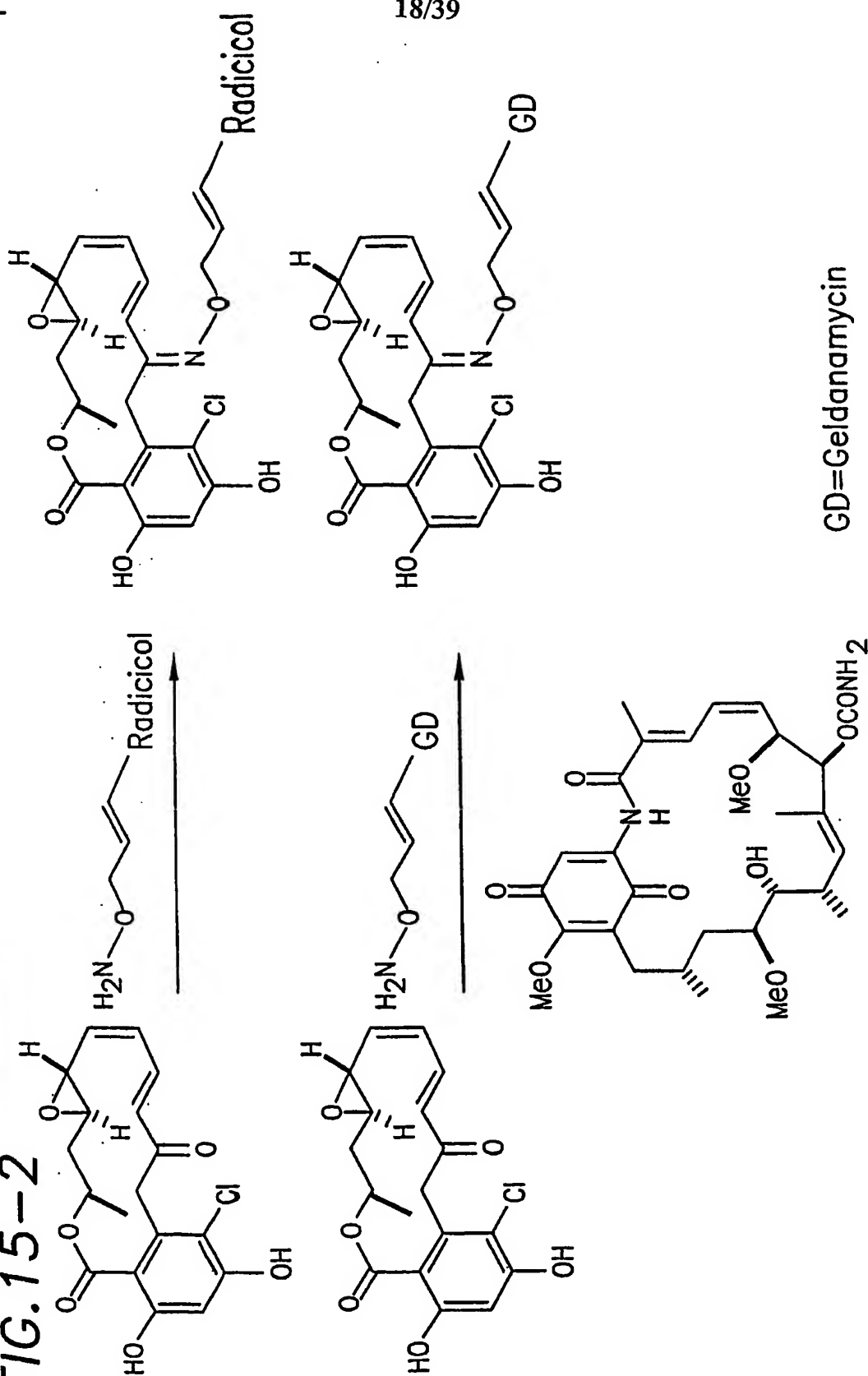
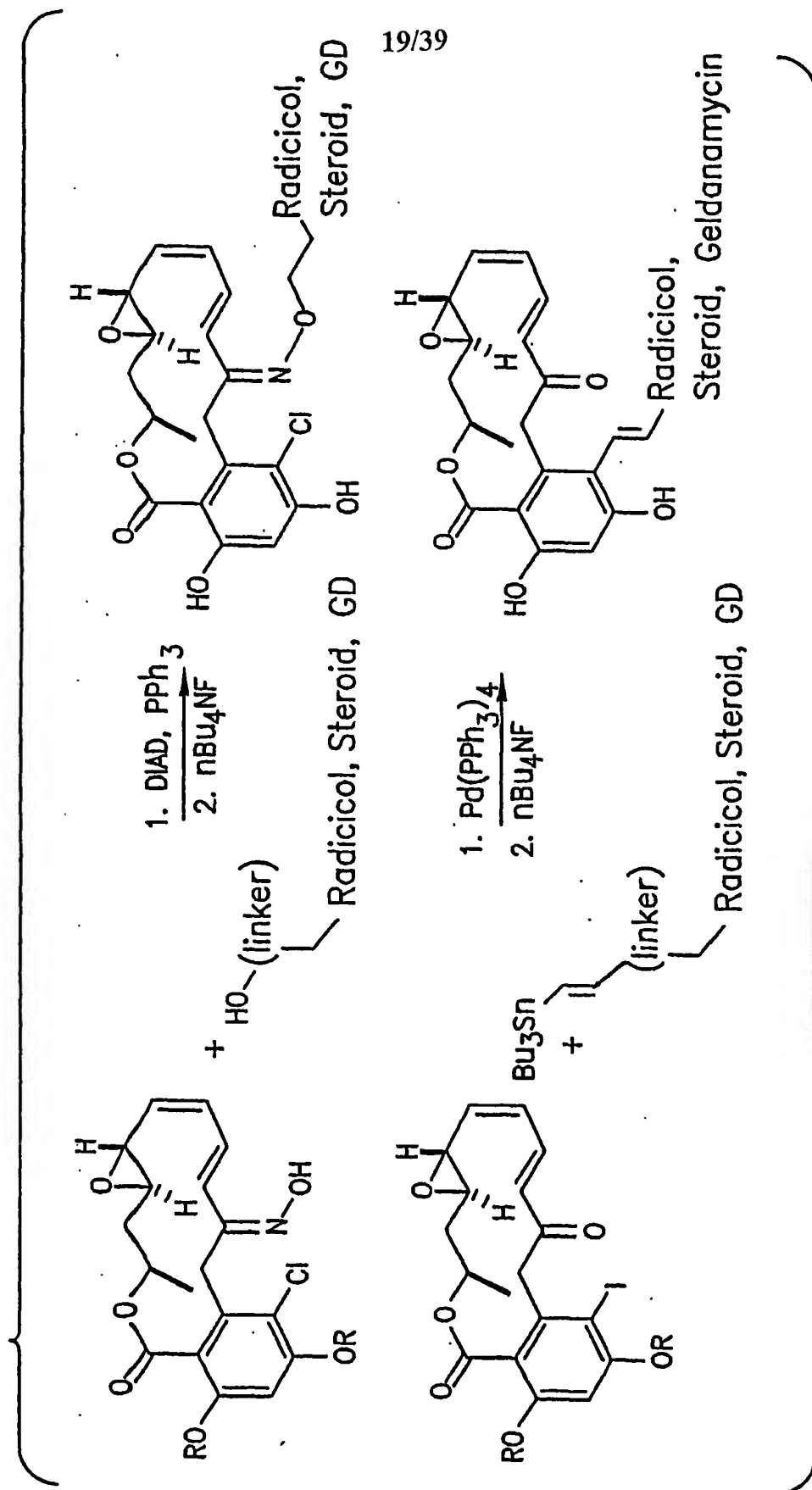


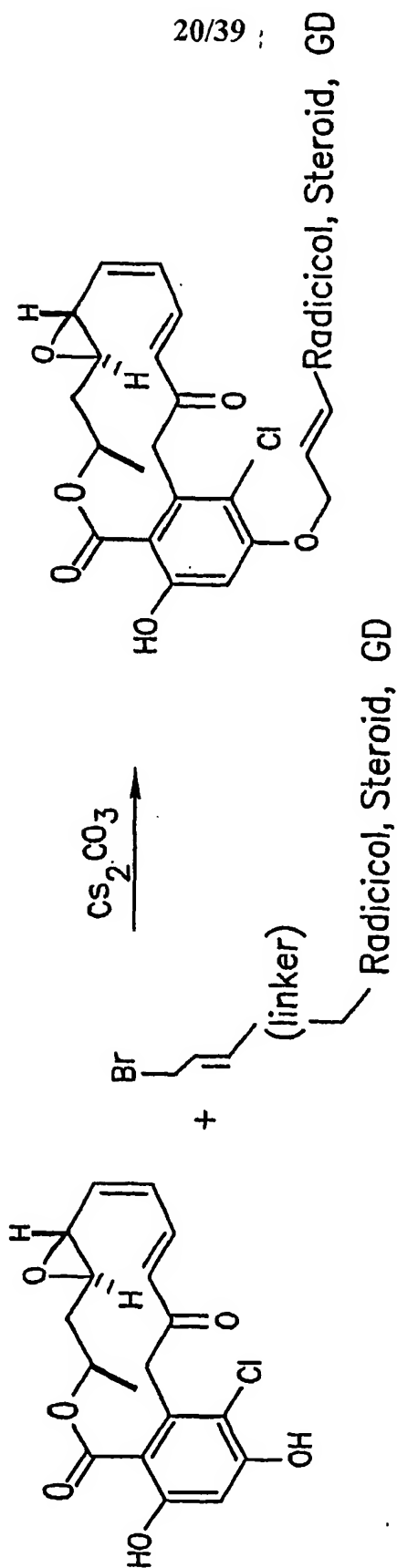
FIG. 16-1



TO FIG. 16-2

FROM FIG. 16-1

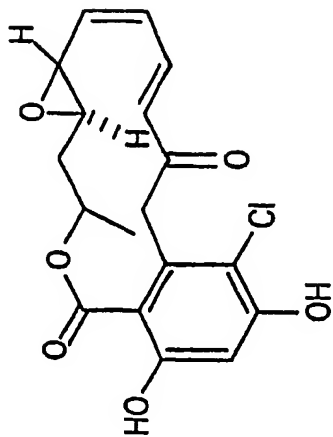
FIG. 16-2



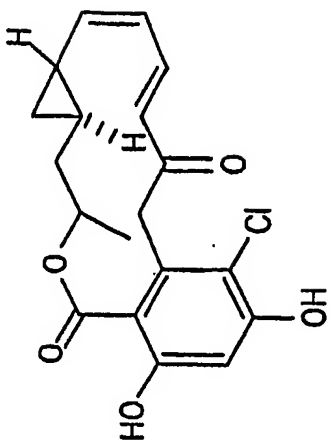
21/39

FIG. 17-1

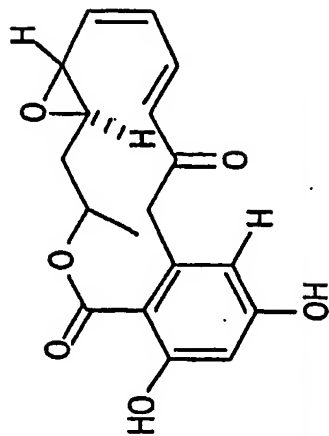
I. Radical



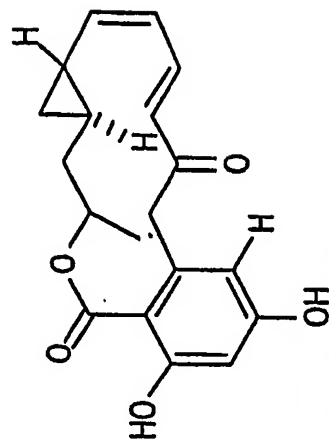
III. Cyclopropyl radical



II. Monocillin I



IV. Cyclopropyl monocillin

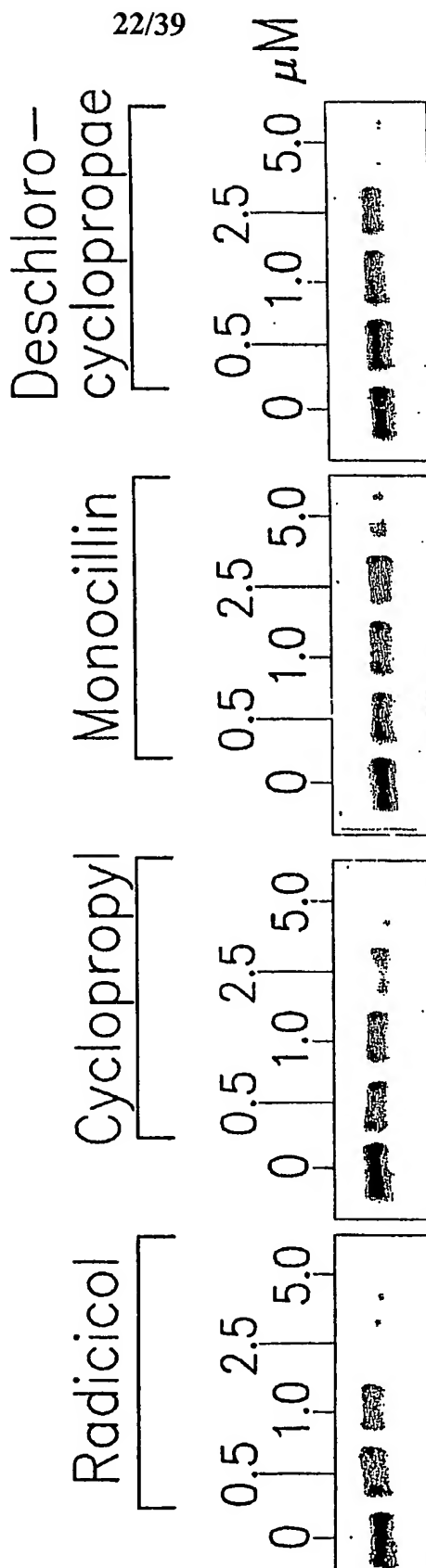


TO FIG. 17-2

FROM FIG. 17-1

FIG. 17-2

MCF7 Cells Treated with Radicicol and Analogues



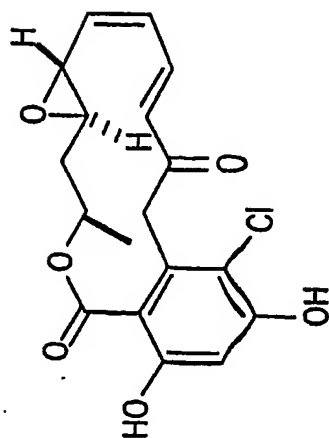
HER2

TO FIG. 17-3

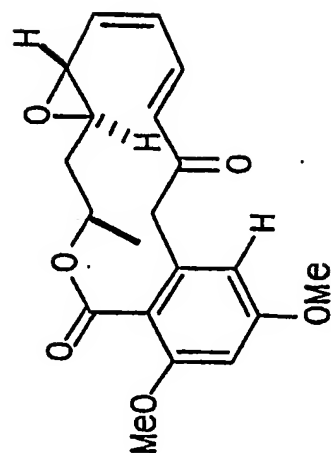
FROM FIG. 17-2

FIG. 17-3

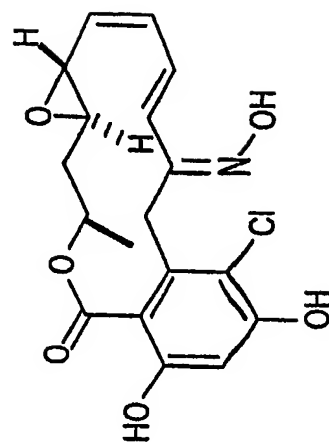
I. Radical



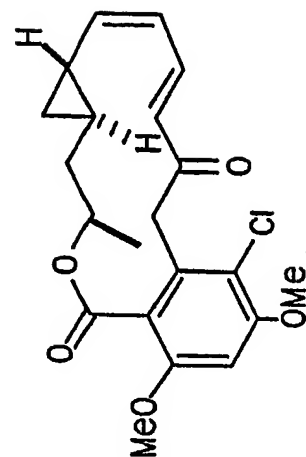
V. Dimethyl Monocillin I



VII. Radical Oxime



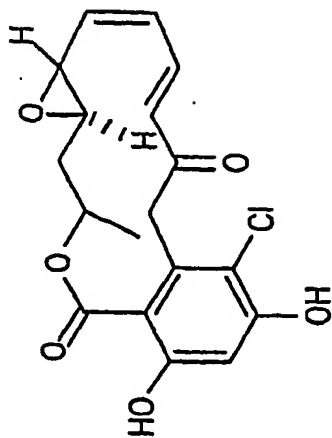
VI. Dimethyl Radical



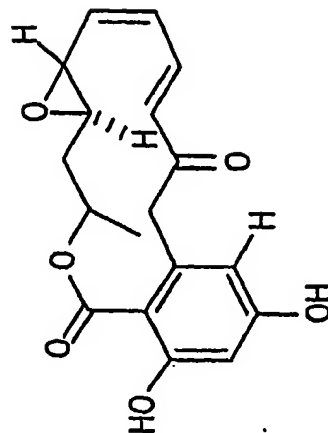
24/39

FIG. 18-1

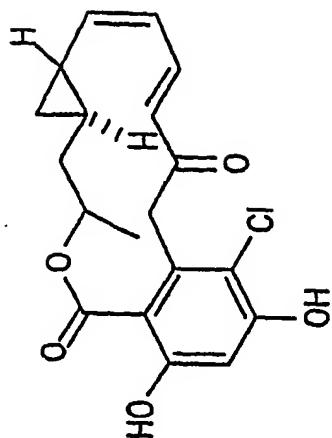
I. Radicicol



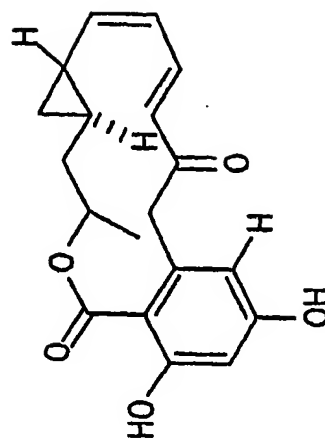
II. Monocillin I



III. Cyclopropyl radicicol



IV. Cyclopropyl monocillin



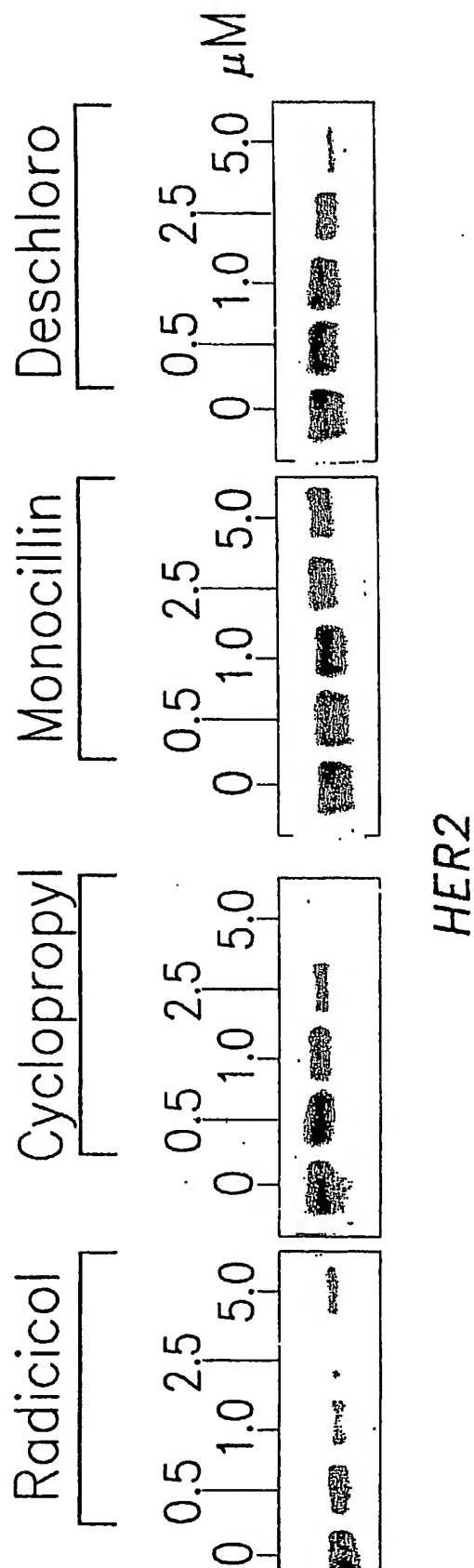
TO FIG. 18-2

25/39

FROM FIG. 18-1

FIG. 18-2

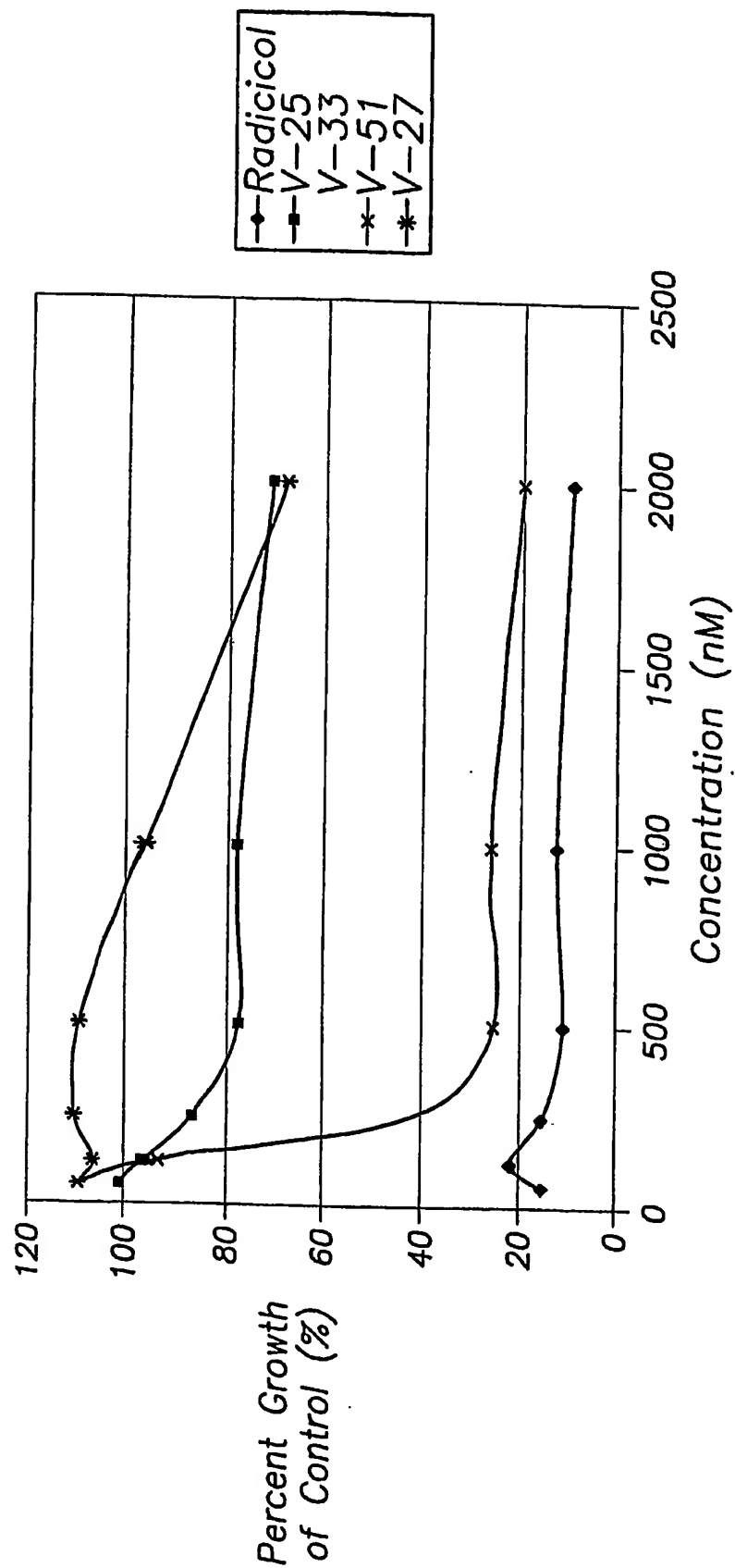
BT474 Cells Treated with Novel Radicicoli (24hrs.)



26/39

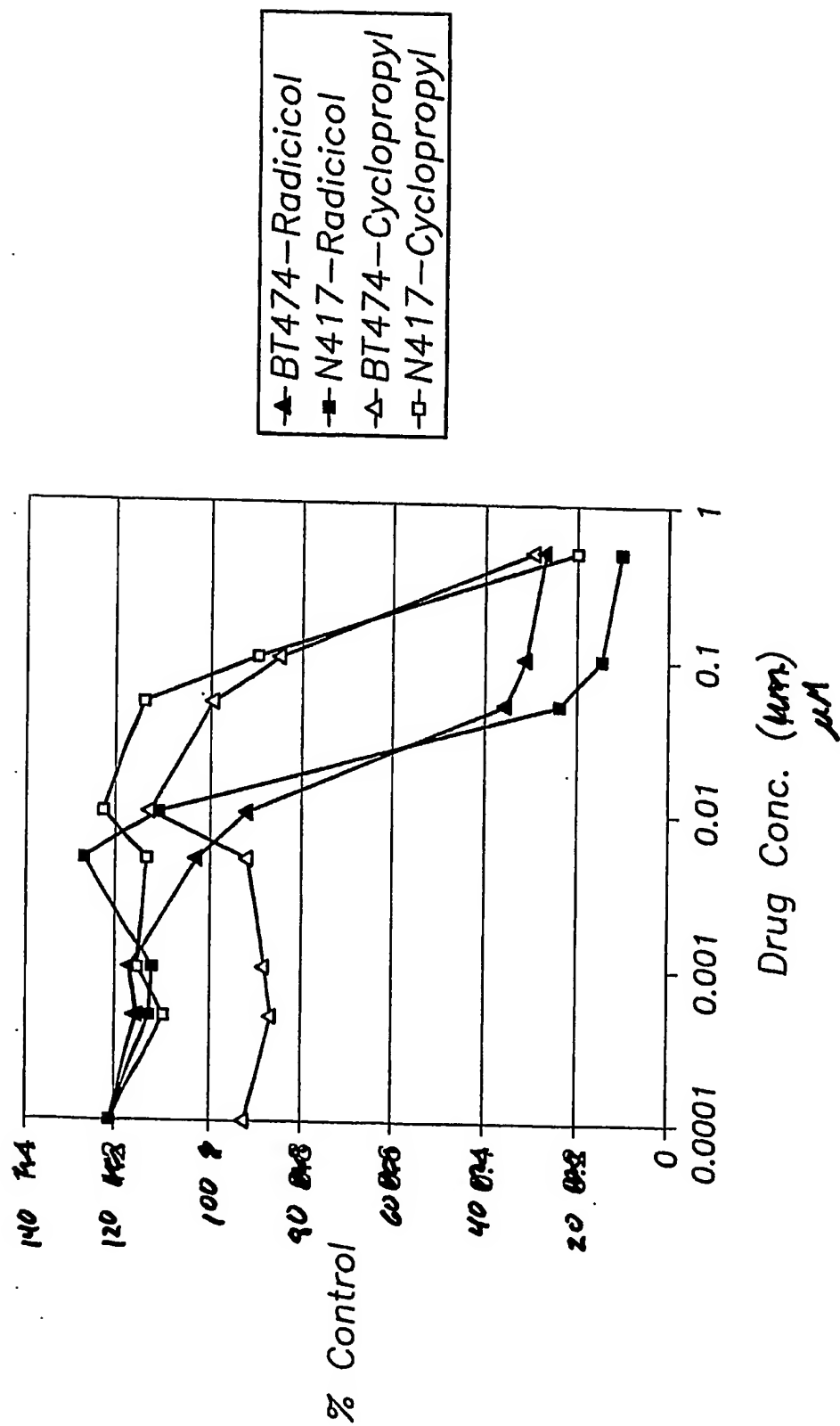
FIG. 19

Growth of MCF7 Treated with Radical and Derivatives of Radical

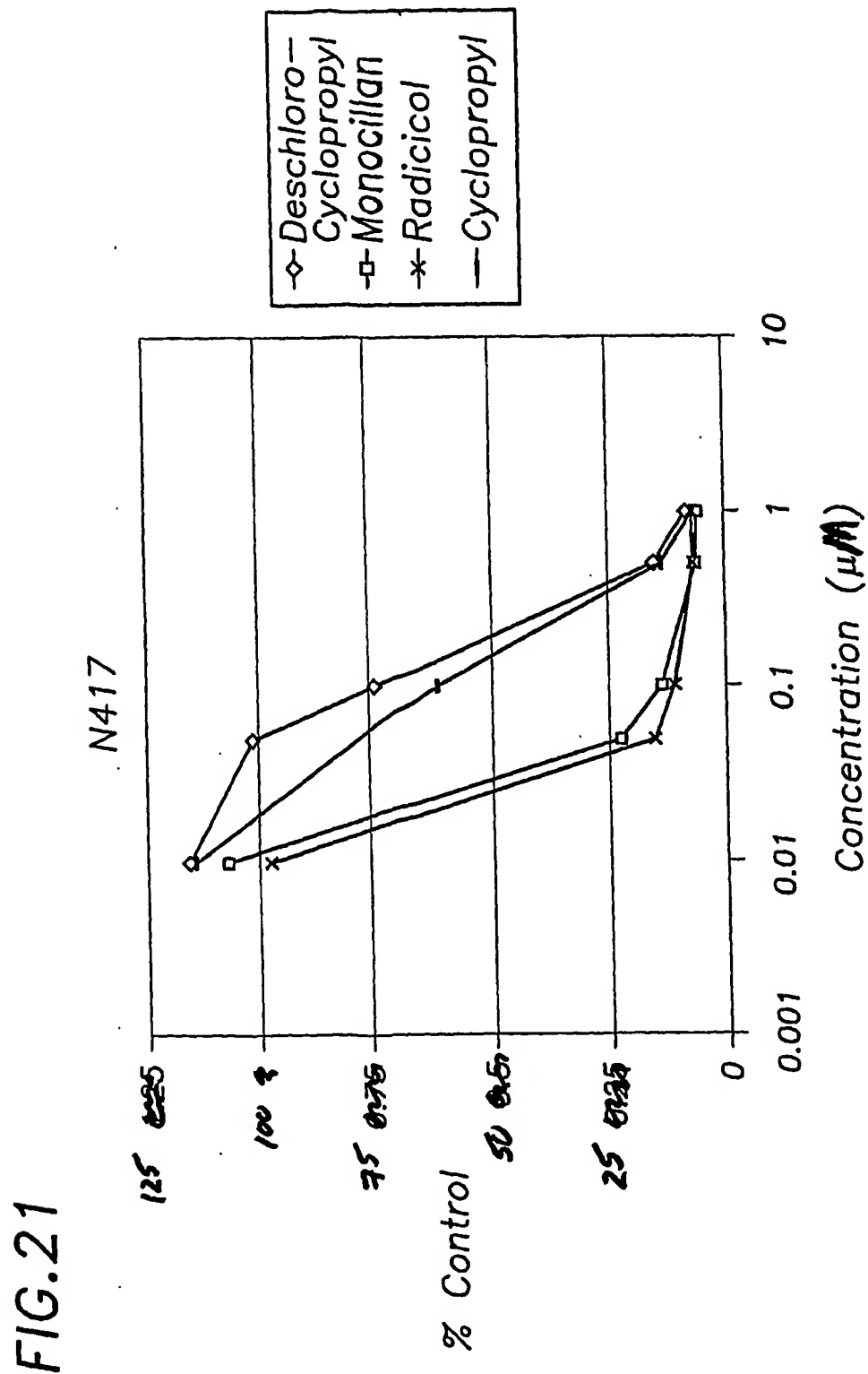


27/39

FIG. 20



28/39



Therapeutic effect of Cycloproparadicol in nude mice bearing human mammary carcinoma MX-1 xenograft (Q2Dx6, iv.injection)

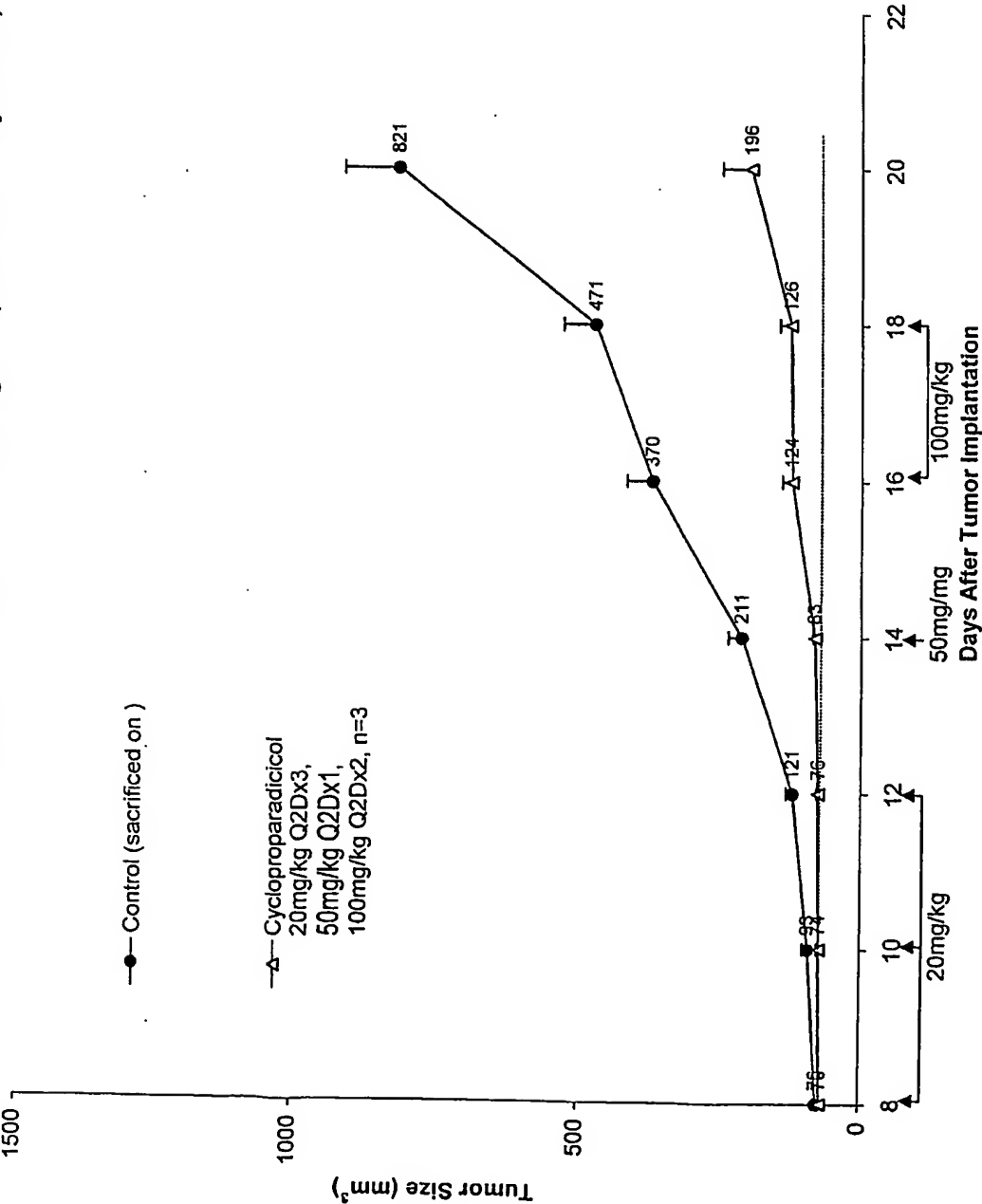


Fig. 22

Body weight changes of nude mice bearing human mammary carcinoma MX-1 xenograft:
Treatment with Cycloproparadicol (Q2Dx6, iv.injection)

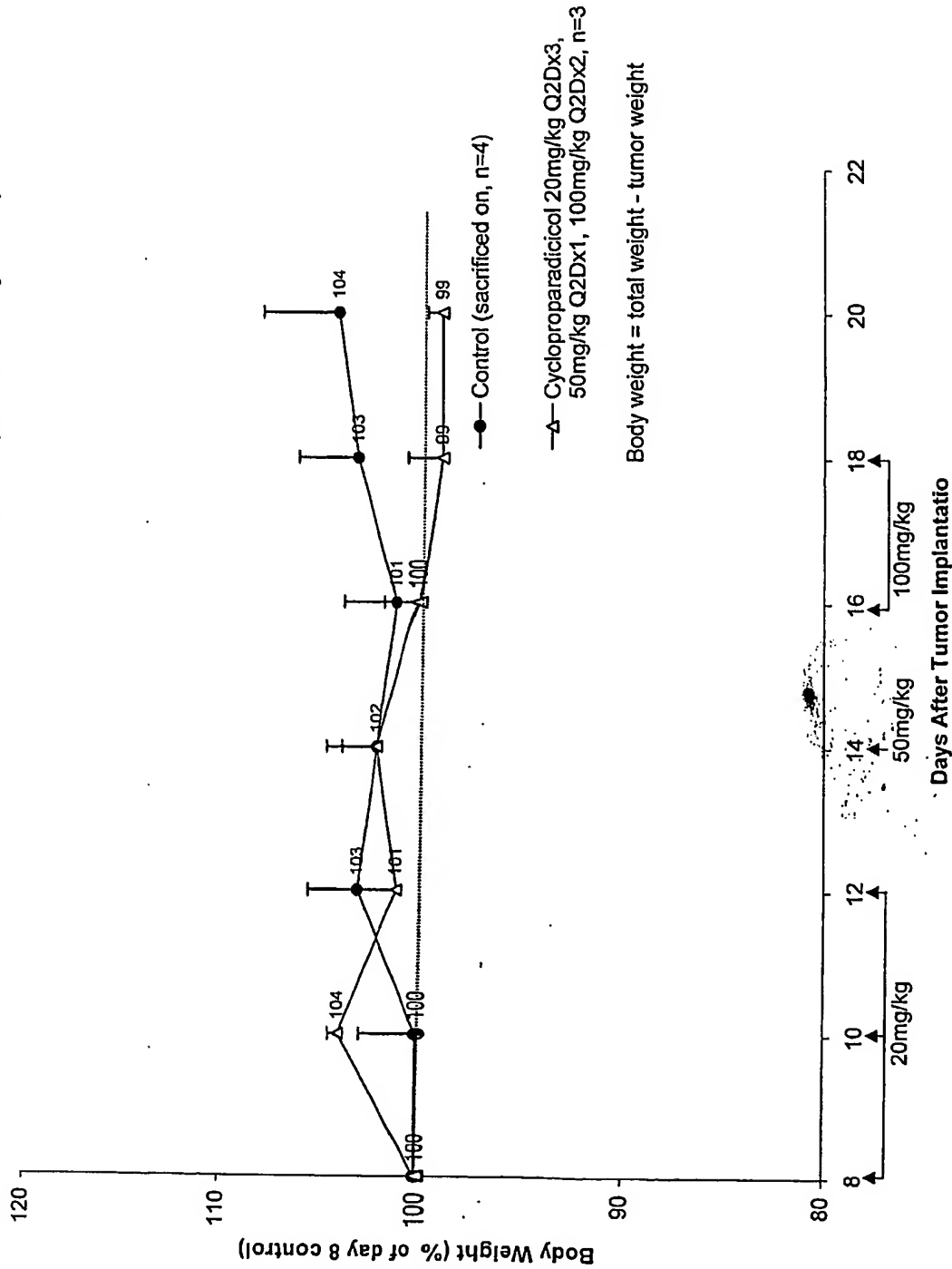


Fig 23

31/39

Therapeutic effect of Radicolol & Cycloproparadicol in nude mice bearing human colon carcinoma (HCT-116) xenograft (QDx7, 4hr. iv-infusion)

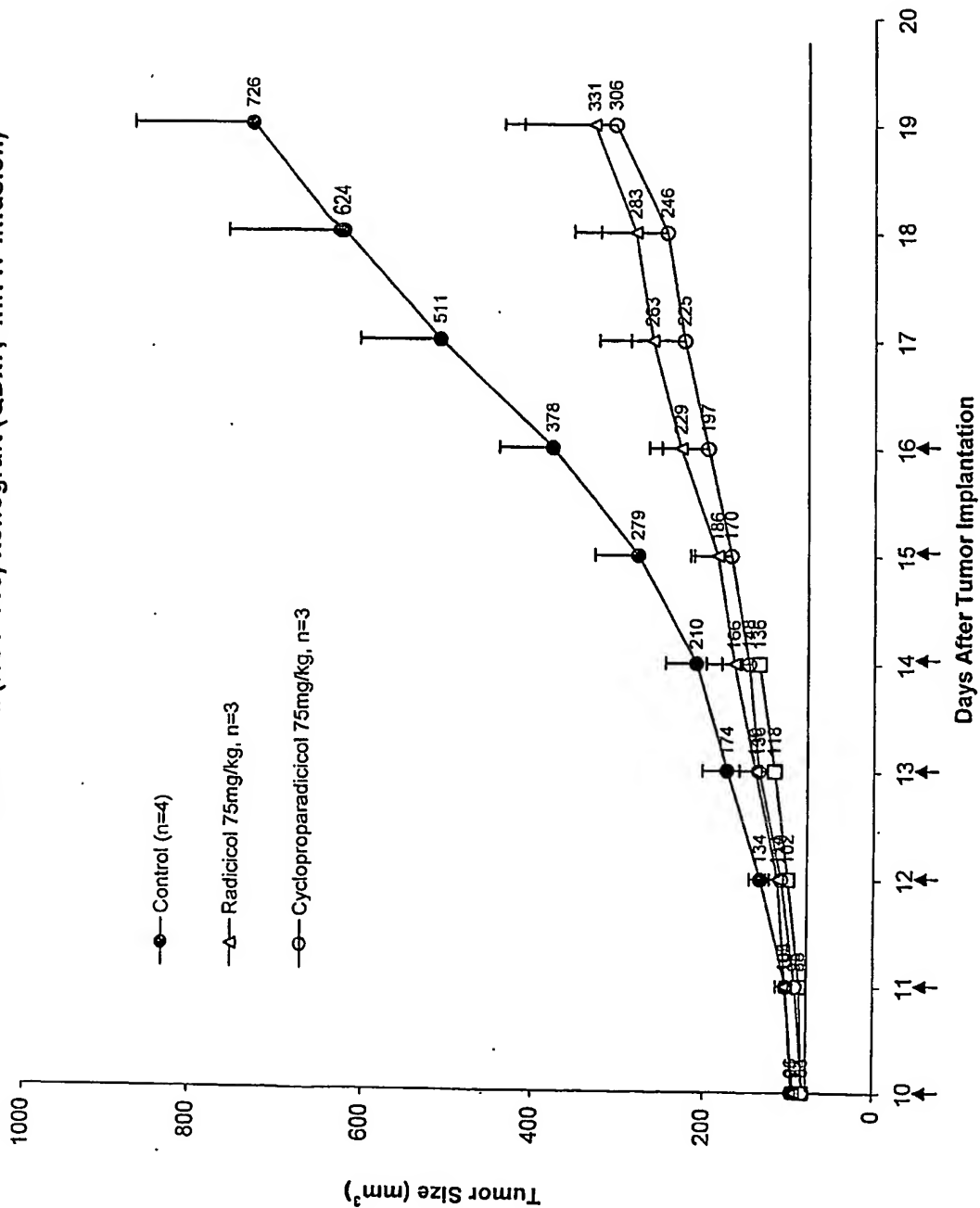


Fig. 24

32/39

Body weight changes of human colon carcinoma (HCT-116) xenograft bearing nude mice following treatment with Radicolol & Cycloproparadicolol (QDx7, 4hr. iv-infusion)

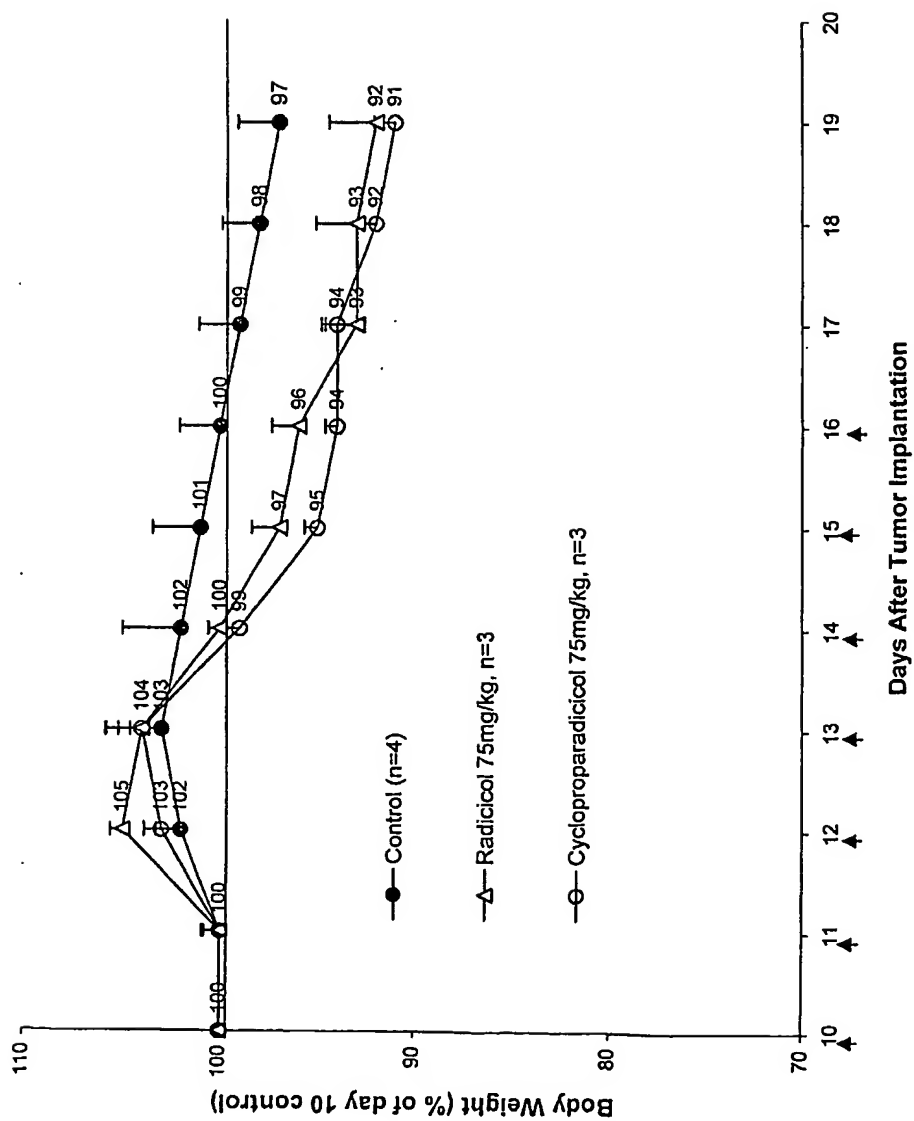


Fig. 25

MX-1 tumors
12 hrs following a 6 hr CIVI



Fig. 26

34/39

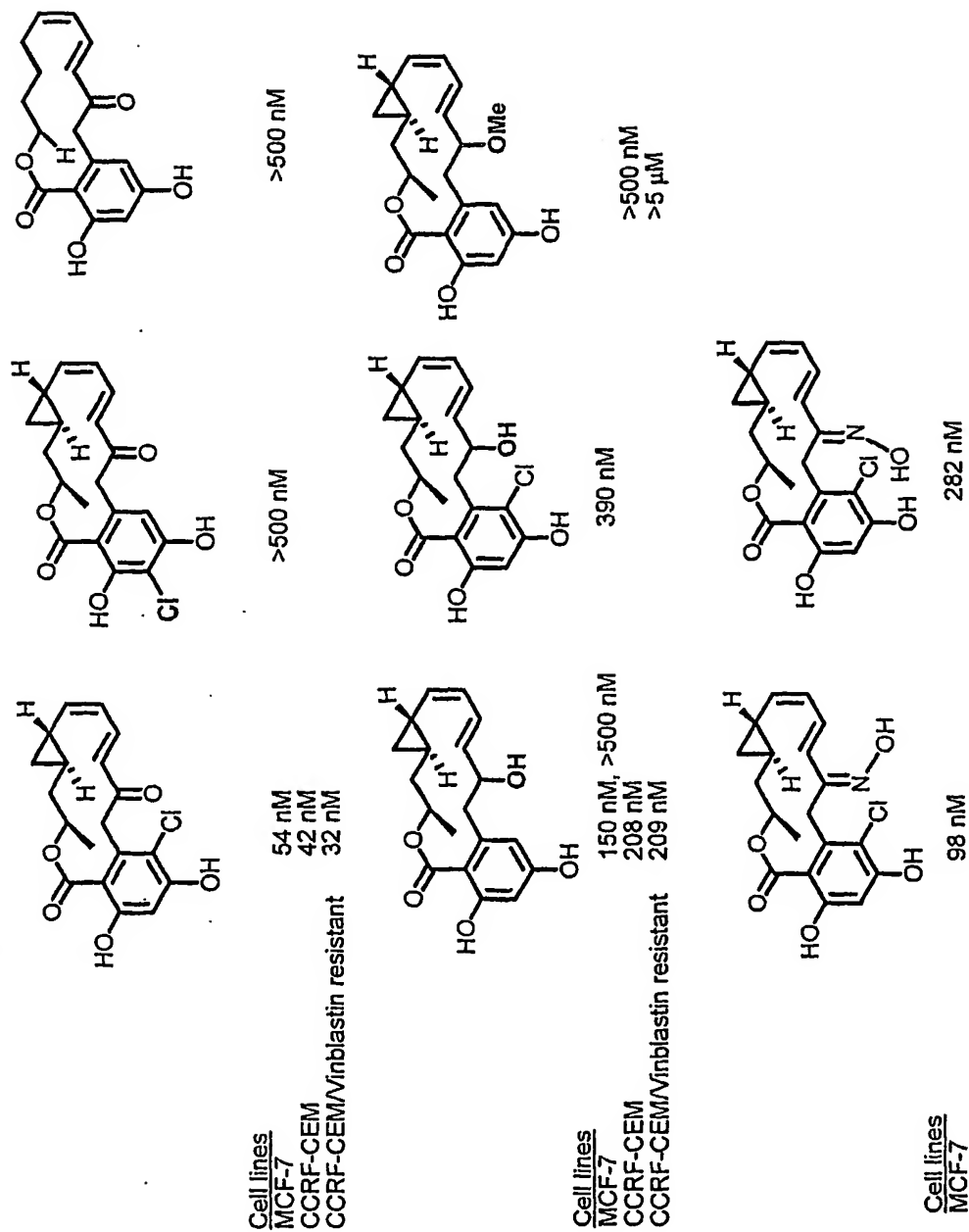
IC₅₀ of Growth Inhibition of Different Tumor Cell lines

Fig. 27

Degradation of HER2 by
Cycloproparadicicol Analogues

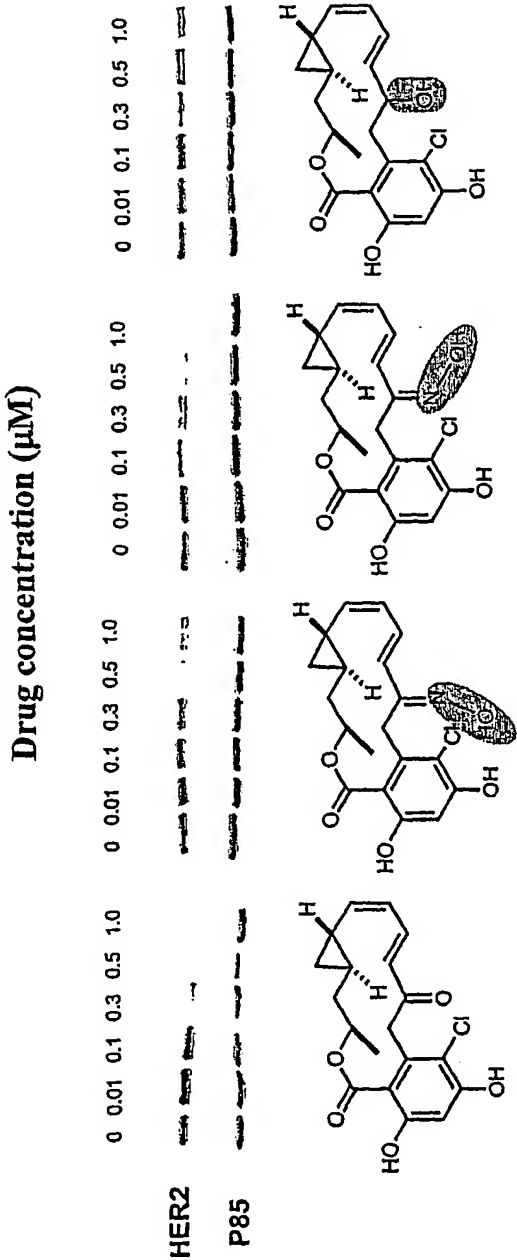


Fig. 28

36/39

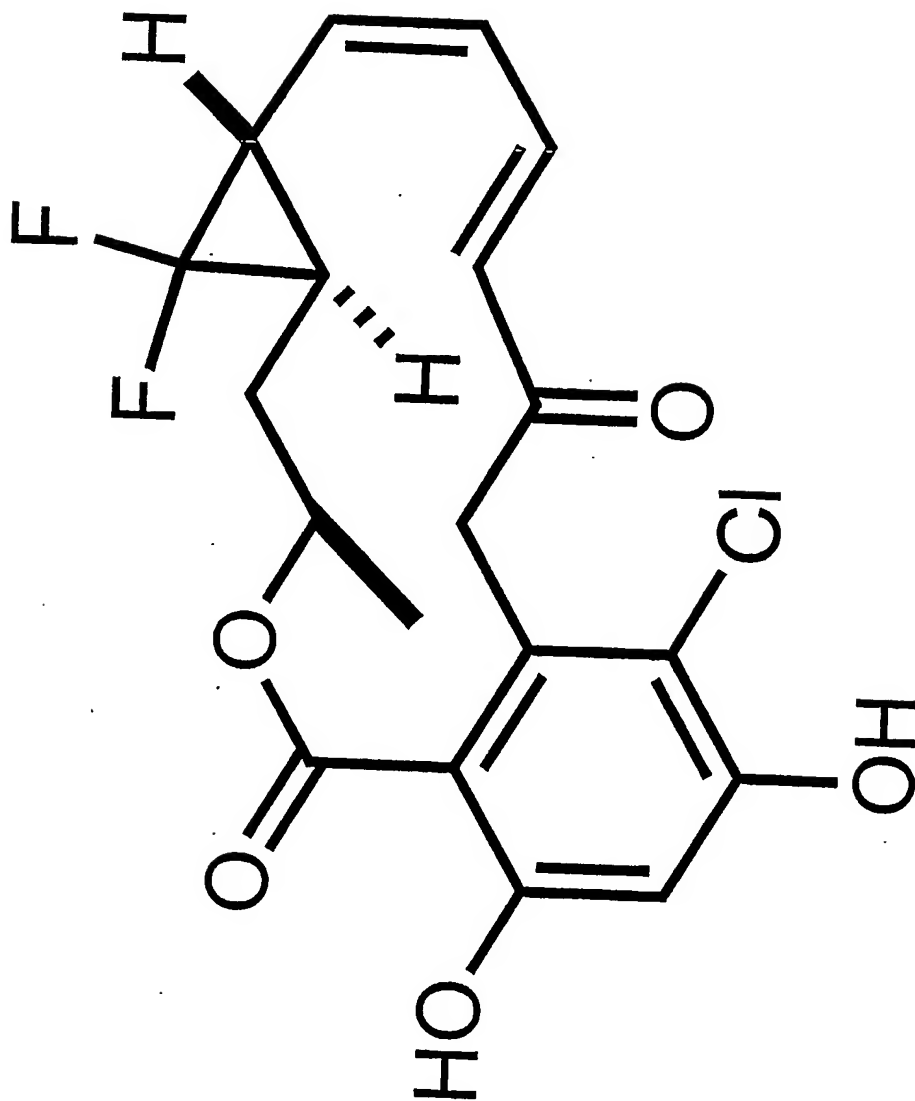


Fig. 29

Cytotoxic effect on CCRF-CEM cell growth by radicicol analogs^a.

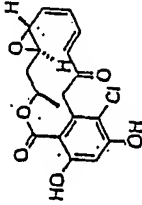
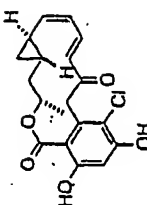
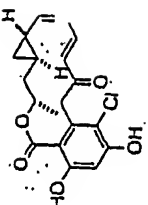
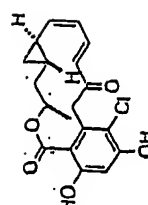
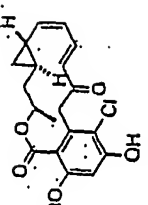
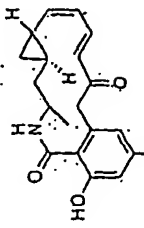
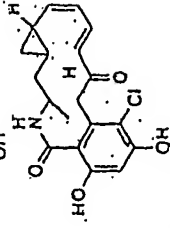
Compound	Structure	Cell growth inhibition (IC ₅₀ in μ M) ^b		
		CCRF-CEM	CCRF-CEM/VBL ^c	CCRF-CEM/taxol ^c
Radicicol (Sigma)		0.055 \pm 0.03	0.099 [1.8x]	0.070 [1.3x]
Cyclopropyl 1		4.81	9.84 [2.0x]	7.74 [1.6x]
Cyclopropyl 2		2.34	4.89 [2.1x]	2.89 [1.2x]
Cyclopropyl 3		0.58 \pm 0.13	0.87 [1.5x]	0.53 [0.9x]
Cyclopropyl 4 (Cycloproparadicicol)		0.055 \pm 0.04	0.041 [0.75x]	0.070 [1.3x]

Fig. 30A

38/39

Cytotoxic effect on CCRF-CEM cell growth by radicicol analogs^a. (Cont'd)

Compound	Structure	Cell growth inhibition (IC ₅₀ in μ M) ^b		
		CCRF-CEM	CCRF-CEM/VBL ^c	CCRF-CEM/taxol ^c
DechloroCyclopropa- radicicol Lactam		>10	>10	ND
Cycloproparadicicol Lactam		>5	>5	ND

^a Compounds of radicicol and cycloproparadicicol stereoisomers.

^b Cell growth inhibition was measured by XTT tetrazolium assay after 72-hour incubation for cell growth. (Chou et al., Proc. Natl. Acad. Sci. USA 95: 15798-15802, 1998). Five to eight concentrations for each drug were used. IC₅₀ values were determined from dose-effect curves by using a computer program CalcuSyn for Windows by Chou and Hayball (Biosoft, Cambridge, UK, 1997).

^c CCRF-CEM/VBL and CCRF-CEM/taxol are the CCRF-CEM sublines that are 320-fold and 42-fold resistant to vinblastine and taxol, respectively. Number in brackets is the fold of resistance of each drug when comparing the IC₅₀ values with those of the parent cell line, CCRF-CEM. The results showed that radicicol and cycloproparadicicol stereoisomers are not cross-resistant to vinblastine (typical MDR-Pgp substrate) nor to Taxol.

Fig. 30B

39/39

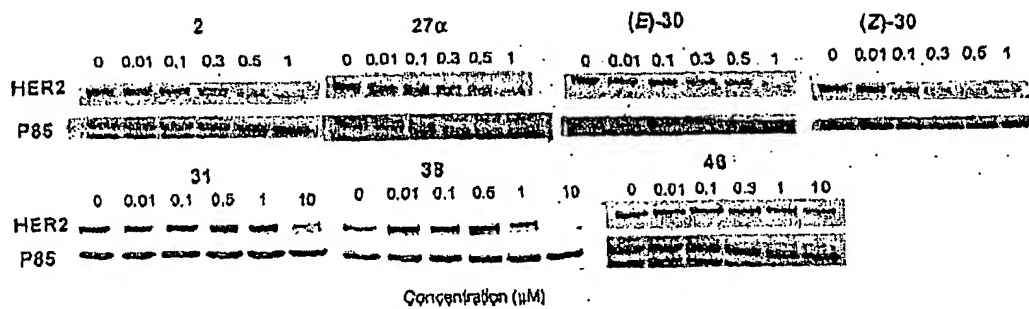


Figure 31: Her2 Degradation Assay